Chapter

Gas Sensors Based on Conducting Polymers

Nagy L. Torad and Mohamad M. Ayad

Abstract

Since the discovery of conducting polymers (CPs), their unique properties and tailor-made structures on-demand have shown in the last decade a renaissance and have been widely used in fields of chemistry and materials science. The chemical and thermal stability of CPs under ambient conditions greatly enhances their utilizations as active sensitive layers deposited either by in situ chemical or by electrochemical methodologies over electrodes and electrode arrays for fabricating gas sensor devices, to respond and/or detect particular toxic gases, volatile organic compounds (VOCs), and ions trapping at ambient temperature for environmental remediation and industrial quality control of production. Due to the extent of the literature on CPs, this chapter, after a concise introduction about the development of methods and techniques in fabricating CP nanomaterials, is focused exclusively on the recent advancements in gas sensor devices employing CPs and their nanocomposites. The key issues on nanostructured CPs in the development of state-of-the-art miniaturized sensor devices are carefully discussed. A perspective on next-generation sensor technology from a material point of view is demonstrated, as well. This chapter is expected to be comprehensive and useful to the chemical community interested in CPs-based gas sensor applications.

Keywords: conducting organic polymers, gas sensors, polypyrrole (PPY), polyaniline (PANI), toxic gases, miniaturized sensor devices

1. Introduction

The initial development of conducting polymers (CPs) began in 1977 by the American scientists MacDiarmid and Heeger and their Japanese colleague Shirakawa, as they discovered a highly conductive polyacetylene (PA) via chemical doping with iodine or other ionic dopants which endowed the polymer with metal-like properties, producing copper-colored films with an increased conductivity of 10 orders of magnitude (Noble Laureate in Chemistry in 2000) [1–3]. However, the instability and ease of degradation of PA by oxidative degradation was a big obstacle to find applications such as batteries or electronic devices. Since then, there have been worldwide considerable efforts in synthesizing numerous other CPs similar to those of PA with high doping level over the range from insulator to metal, such as polyphenylene (PP), polypyrrole (PPY), polythiophene (PTH), and polyaniline (PANI) [4–7].

Hitherto, however, studies on CPs have been extensively investigated in both fundamental and practical perspectives; their unique chemical and physical characteristics have been continuously discovered. These fascinating properties are derived from their π-electron conjugation system along the polymer chain, which allow

the formation of delocalized electronic states, resulting in a resonance-stabilized structure of the polymer [8]. Over a wide range of polymer-based materials, CPs are of particular interest due to their unique electrical and optical properties rivaling metals or inorganic semiconductors and still retain the attractive mechanical properties and processing advantages of polymeric materials, known as "synthetic metals" [9]. In addition to a variety of advantages, ease of preparation procedures, controlling the morphology, structural flexibility, light weight, and cost-effectiveness are included. The molecular structures of some of the prominent CPs include PANI, PPY, poly-paraphenylene (PPP), and PTH, which are shown in **Figure 1** (left) in their non-conducting (undoped) states. In the past few decades, CPs have been continuously studied for their tremendous use in electronic and optoelectronic devices. In this context, particular interest has been paid toward utilization of nanostructured CP-based sensors as high-performance signal transducers with enhanced sensing capability relative to their conventional bulk-scale materials, because of their high surface-to-volume ratios and unique electrical and physical properties [10]. In the sense of sensor applications, the distinguishing properties of CPs offer a great potential in efficient sensing systems by virtue of their unique electrical, optical, and mechanical transduction mechanisms [11, 12]. To achieve superior performances in both sensitivity and response time, critical issues include conductivity, morphological design, size control, bioprobes, and surface modification which are very crucial. In terms of conductivity change, oxidation level achieved by chemical and electrochemical doping/dedoping mechanisms could in turn fabricate a sensitive and rapid sensor response to an analyte of interest at room temperature [11, 13]. Recently, special attention has been paid to nanostructured CPs as one of the most substantial achievements in sensor technology because their high surface areas, multidimensional architectures, and easy functionalization with a variety of functional groups enable the sensing of a trace amount of a target species [14]. Further, the signal intensity of the sensor can be enhanced by controlling the shapes because of the one-directional signal pathway of the CP nanostructure.

Typical CPs, such as PPY, PANI, PTH, and poly(3,4-ethylenedioxythiophene) (PEDOT), have been extensively studied in environmental monitoring of various types of target analytes, such as volatile organic compounds (VOCs), gases, heavy metals, and biomolecules [15–17]. On exposure to analyte, their response mechanisms comprise chemical and physical interactions, including oxidation/reduction, swelling, conformational changes, charge transfer, and so on. In terms of charge

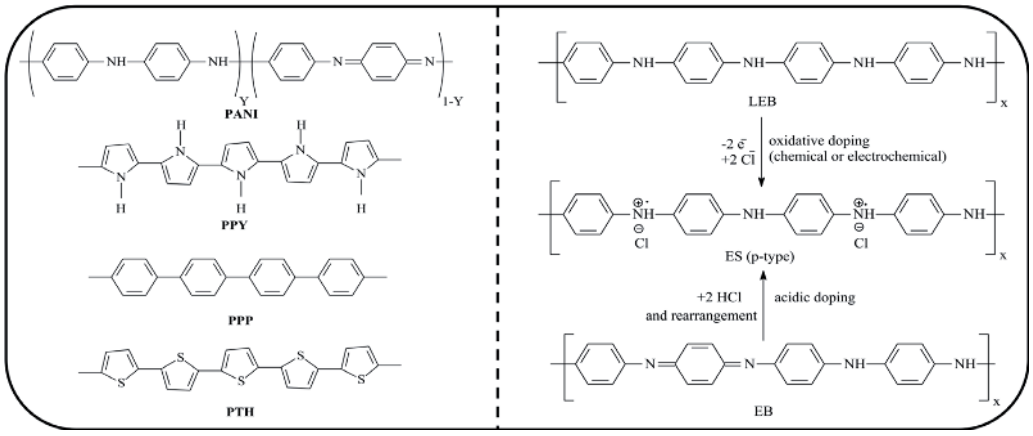

Figure 1.
(Left) Representative of typical molecular structures of CPs and (right) illustration of doping mechanisms of PANI. The terms "LEB and ES" represent the completely reduced form of colorless PANI called "leucoemeraldine base" and the highly conducting emeraldine salt (ES) obtained by chemical reaction with protonic acids whose color is green, and the conductivity is around 15 S·cm^{-1}.

transfer, doping and oxidation levels and conjugation length are key intrinsic factors of CPs in which the delocalization of the π-electron takes place. It is well-known that most of CPs are p-type semiconductors, and thus they feature the emergence of charge carriers (polaron and biopolaron) as oxidative doping proceeds as shown in **Figure 1** (right). Accordingly, these intrinsic factors are very useful for designing the high performance of CP-based sensors.

2. Synthesis of nanostructured conducting polymers

Conducting polymers have traditionally been synthesized either by chemical or electrochemical oxidation routes of the corresponding monomers with acid or peroxide initiators resulting in insulating materials that require a post-doping process [11, 18–20]. In both cases, the overall polymerization process includes the oxidation of monomer, followed by coupling reaction of the charged monomers to produce a polymer chain. Chemical polymerization method is usually applicable for large-scale production of CP powders. In contrast, electrochemical polymerization offers an in situ one-step effective process for producing CP nanomaterials deposited onto the electrode surface as films for a sensor device, which grow along the direction of the electric field to form oriented nanostructures. The morphological structure and thickness of the CP films can be tailored by controlling the electrochemical polymerization conditions, applied potential or current density, and electrolyte. Owing to their electrical conductivity, CPs can grow electrochemically on an electrode surface without addition of oxidizing agents.

Great efforts have been devoted toward the preparation of CP nanomaterials for the fabrication of miniaturized novel flexible sensor platforms that enable portability and high-density arrays because of using small sample amounts, which offer excellent prospects in sensor nanotechnology for advanced detection systems [21]. Recent studies have demonstrated the synthesis of nanostructured CPs with controlled shape and size, which ranged from lithographic techniques to chemical methods [22–33]. Stejskal and coworkers demonstrated synthesizing PANI nanostructures and its derivatives by the chemical oxidative polymerization in water [34–36]. Further, Ayad et al. reported the synthesis of PANI and PPY nanotubes, nanorods, nanoflowers, nanoflakes, and nanocomposites via chemical oxidative polymerization using diluted aqueous camphor sulfonic acid (CSA) and acetic acid solutions as shown in **Figure 2** [37, 38]. Besides, the incorporation of metals/metal oxide NPs, graphene, or carbon nanotubes (CNTs) into nanostructured PANI and PPY has been recently reported as a way of increasing the CP electrochemical and electrocatalytic activities and sensing capabilities [39–42].

Recently, research studies have focused on the development of templating approaches such as hard template, soft template, and template-free synthesis as an aid template in combination with other polymerization methods, like dispersion polymerization, interfacial polymerization, vapor deposition polymerization (VDP), and electrochemical polymerization for the synthesis of well-defined CP

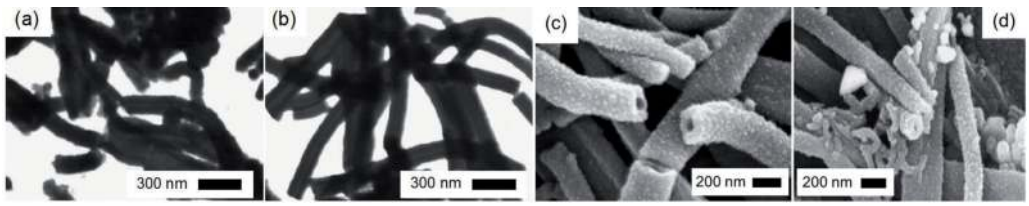

Figure 2.
(a and b) STEM of PANI salt and PANI base prepared with CSA, respectively. (c and d) SEM images of nanotubular PANI and PANI/Ag nanoparticles, respectively, prepared using chemical oxidative polymerization in acetic acid (adapted with permission from Ref. [37, 38] Copyright 2009, Elsevier).

nanomaterials [43–48]. Depending on the monomer properties, whether it interacts electrostatically or chemically bound to the template, different CP micro- and nanostructures can be fabricated retaining the original shape of the porous template itself.

So far, the hard template approach is utilized for the synthesis of one-dimensional (1D) CP nanostructures such as nanotubes, nanorods, and nanofibers which are synthesized using anodic aluminum oxide (AAO) membranes, zeolite channels, mesoporous silica, and track-etched polycarbonate [49, 50]. Depending on the pore length and diameter of the membrane template, size and diameter of CP nanostructures can be precisely controlled because the monomers are absorbed or attached inside the pore walls, followed by chemical oxidative polymerization [51]. In addition, the wall thickness can be tuned by controlling the polymerization time and concentration of monomer. In pioneering studies to Jang et al., they proposed a facile route to synthesize PPY nanotubes with a wall thickness of a few nanometers using AAO membrane template via VDP as signal transducers [52, 53]. Park et al. reported a one-pot synthesis of Ag NPs decorated PEDOT nanotubes with high surface area and enhanced conductivity via VDP method using an AAO template and $Fe(NO_3)_3$ as an oxidant for sensing ammonia gas [54]. Furthermore, combination of electrospinning using electrospun nanofiber templates and VDP methods provided CP nanomaterials with remarkable surface areas and uniform nanostructures [55]. Kwon et al. reported the use of electrospun ultrathin poly(methyl methacrylate) (PMMA) nanofibers as a template to synthesize PEDOT after immersing with ferric chloride solution followed by VDP of EDOT monomer at controlled temperatures and pressures to yield core-shell PEDOT nanofibers [56]. However, this method suffers from the difficulties of removing the template without aggregation of the resulting CPs and is not suitable for commercial applications. Regardless, high-impact nanostructured CP composites can be prepared without removal of template. Furthermore, previous studies reported that the synthesis of different CP nanohybrids, such as metal, metal sulfides, and metal oxides/PPY nanowires, was prepared by the hard template method [57–59].

An alternative strategy known as the soft template approach has been used to effectively fabricate CP nanomaterials using templates such as surfactants, block copolymers, polyelectrolytes, and liquid crystals combined with interfacial polymerization and emulsion/dispersion polymerization [60–62]. Accordingly, 1D CP nanostructures can be tailored by varying the synthetic conditions and produced in large scale [63]. A cationic surfactant, dodecyltrimethylammonium bromide (DTAB), has been utilized to form spherical micelles reinforced with decanol in aqueous solution as a stable microemulsion for the synthesis of monodispersed PPY nanoparticles with a large quantity [64]. However, this technique requires high surfactant concentration, which is problematic in terms of cost and environmental pollution. Jang and coworkers reported the formation of PPY nanotubes and nanoparticles using a reverse micelle system (water-in-oil systems) with a molecular template, sodium bis(2-ethylhexyl) sulfosuccinate (known as AOT), and dispersion polymerization (water-soluble polymers) employing polyvinyl alcohol (PVA) in an aqueous solution, respectively [65–67]. In addition, PANI nanowire network was carefully synthesized using a cationic surfactant, hexadecyltrimethylammonium bromide and oxalic acid in aqueous solution [68]. Further, an anionic oxidant/cationic surfactant complex was used as a template to fabricate clip-like nanostructures of PPY, PANI, and PEDOT [69]. By judiciously changing the combination of surfactants, oxidizing/doping agents, pH, and temperature, infinite nanostructures with desirable morphology could be successfully fabricated. A facile method to synthesize nanostructured core-shell PPY/Ag using sodium dodecyl benzyl sulfonate (SDBS) and CTAB as templates through a redox reaction was proposed [70]. Very recently, Stejskal et al. demonstrated a cotton fabric coating of PPY and PANI nanotubes, colloidal PPY nanotubes/nanorods, and microporous PANI cryogels obtained by the chemical polymerization

of pyrrole in the presence of a structure-directing dye, methyl orange (MO), as a starting template, and poly(*N*-vinypyrrolidone) (PVP), respectively [71–78]. The interaction between starting materials and dye was expected to produce a template, which is further used for the growth of CP nanotubes. After the addition of oxidant, MO itself in its acid form has limited solubility which may serve as a starting template and the growth of nanotubes may proceed beyond the template [79, 80]. Also, the partial solubilization of MO-$FeCl_3$ template in the presence of CTAB was an effective way to fabricate PPY nanotubes having smaller diameter by reactive self-degrade template method [81, 82]. In addition, ionic liquid template-assisted synthesis of PANI/AgCl and PPY/Ag nanocomposites has recently been conducted by the direct oxidation of pyrrole by silver cations from silver bis(trifluoromethanesulfonyl)imide ($AgTf_2N$), using 1-butyl-3-methylimidazolium bis(trifluoromethylsulfonyl)imide ($BMImTf_2N$) as solvent and template [83, 84]. Moreover, dual-template approach involving an AAO template and surfactants was also applied by another research group for fabricating nanotubular PPY [85].

Template-free approach is a quite facile and a straightforward method for producing CP nanomaterials with large quantity without using specific sacrificial templates and post−/pretreatment procedures; however extensive efforts are needed to design building blocks that can spontaneously self-assemble into nanostructures under certain conditions without addition of artificial templates. PANI nanofibers prepared from template-free synthesis have been considered as an interesting sensing material since the pioneering study by Huang et al. [86]. Several types of template-free methods, such as chemical, electrochemical, dispersion, and aqueous/organic interfacial polymerization, resulting in various CP micro−/nanostructures, including nanotubes, nanofibers, hollow nanoparticles, core-shell nanoparticles, and multidimensional nanotubes, were extensively reported [87–96]. In addition, a template-free site-specific electrochemical method was developed for the fabrication of PPY, PANI, and PEDOT nanowires on microelectrode junctions [97, 98]. Moreover, a bottom-up approach was applied for the fabricating of PPY/Ag core-shell nanoparticles with an average core diameter of 36 nm and a shell thickness of 13 nm via a simple one-pot synthesis using a starch [99]. In this process, the OH^- groups of the soluble starch provided nucleation sites for Ag^+ that were readily reduced by the pyrrole monomer. Simultaneously, pyrrole monomers were oxidized to form radical cations that have led to the generation of PPY short chains which are further oxidized by the silver nanoseed active sites to finally produce PPY core-shell nanostructures.

3. Gas sensors based on CPs

Chemical sensor is composed of a sensitive material to a particular analyte (molecular recognition) and a transducer, which transforms the concentrations of an analyte into other detectable physical signals, such as current, absorbance, or mass (**Figure 3**). Depending on signal transduction, gas sensor devices based on CPs have been classified by IUPAC [100]. Sensors based on chemical modulation of electronic, optical, or mechanical transduction mechanisms of CPs will be discussed in detail in light of the gas sensing applications.

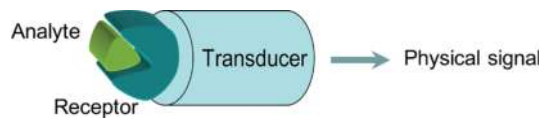

Figure 3.
Illustration of a chemical sensor. (modified and adapted with permission from Ref. [103]. Copyright 2008, MDPI).

3.1 Electrochemical device sensors

Electrochemical devices transform the electrochemical interaction that occurred at analyte-electrode interface into a detectable signal related to the analyte involved in the chemical process. Most of CP sensors rely on electrochemical techniques using amperometric (measurement of current at constant potential) and potentiometric (current measurements during varying potentials). In electrochemical sensor, the charge transport properties of CPs are changed when exposed to an analyte, and the change can be correlated quantitatively to the analyte concentration [101, [102]. In either case, the peak current, as the voltage is scanned, is proportional to the concentration of the target molecule. Based on the electrical transduction modes, electrochemical sensors are classified into the following.

3.1.1 Amperometric sensors

Amperometric gas sensor is a subgroup of electrochemical gas sensing devices that can be utilized for environmental monitoring and clinical analysis of electroactive species, whether in a liquid or a gas phase [102]. The principle of amperometric sensing is to measure the current generated by the redox reaction of an analyte at a working electrode, where the current is subject to Faraday's law and a dynamic reaction, achieving steady-state conditions in the system under an impressed constant voltage on the chemically stable CP-modified electrode [103]. Based on the nature of analyte, when an appropriate potential is applied on the electrode, the analyte molecules are respectively oxidized or reduced on anode or cathode, resulting in a current change. For gas-phase analytes, amperometric sensors are characterized with a gas/liquid/solid boundary and an interfacial transport process that frequently controls the analytical performances and sensor response characteristics. Besides, an inorganic acid is usually used as the supporting electrolyte to provide H^+ ions for ionic conductance in Nafion film. Do et al. fabricated an amperometric NO_2 gas sensor based on PANI/Au/Nafion hybrid nanocomposite using the CV technique at ambient temperature [104]. NO_2 diffusion into a porous PANI was prepared by CV and constant current (CC) methods, resulting in a reduction of mass transfer resistance with increment in cathodic reduction of NO_2 compared to Au/Nafion [105, 106]. Also, the redox response plays a definitive role in the signal transduction of the PANI nanoparticle-based amperometric ammonia gas sensor [107]. The sensor exhibited a sensitivity of 3.04 μA ppm^{-1} with a switching effect for 0 and 100 ppm concentrations. Recent studies have also demonstrated that CNTs enhance the electrocatalytic properties of gases in PANI films associated with the high electron density and conductivity of the polymer and surface reactivity of the composite when used as an amperometric sensor. For example, a 3D nanofibrous structure of WO_3-chitosan-*co*-PANI nanocomposite prepared electrochemically was used for amperometric detection of NO_2 gas in acidic media without interferences using a mineral acid as a supporting electrolyte [108]. The sensor was very highly sensitive enough to low concentrations of NO_2 gas in the range from 100 to 500 ppb, at a pH 2.0 and using 0.25 V *vs* Ag-AgCl. Solid-state amperometric gas sensor based on Nafion/Pt/nanostructured PANI/Au/Al_2O_3 and xerogel Ag/V_2O_5/nanofibrous PANI/Ag hybrids were also investigated for detecting H_2 and NH_3, respectively [109, 110]. The sensitivity and response time for H_2 gas was remarkably promoted by decreasing the Nafion film thickness, and the charge passed for the electrodeposition of Pt and PANI with activity was found to be 338.50 μA ppm^{-1} g^{-1} for measuring 10–10,000 ppm H_2. Upon using xerogel Ag/V_2O_5/nanofibrous PANI/Ag hybrids, the sensor could detect gaseous NH_3 in the range of 0–54 ppm, which would be beneficial for animal confinement husbandry.

3.1.2 Potentiometric sensors

As a subgroup of electrochemical sensors, potentiometric sensors, known as ion-selective or ion-sensitive sensors (ISEs), are utilized for monitoring voltage as a result of specific electrochemical reactions involving a redox reaction for determination of the analyte concentration by measuring accumulation of a charge potential at the working electrode when zero or no current flow arises mainly from shifts in the "dopant" anion equilibrium within the polymer chain (sensing membrane) [111]. Potentiometric sensor technique is very attractive for practical applications, because it provides advantages in the use of small-sized, portable, and low-cost instruments. In the electrochemical cell, the potential (E) arises between two electrodes, defined as the potential difference between the cathodic and anodic potentials typically proportional to the logarithm of the gas analyte concentration which can be estimated from Nernst equation (Eq. (1)).

$$E = E_o + \frac{RT}{nF} lnQ \tag{1}$$

where E_o is the standard electrode potential in volts, R is the universal gas constant (8.314472 J K^{-1} mol^{-1}), T is the absolute temperature in kelvin, F is Faraday's constant (9.648 × 10^4 coulombs mol^{-1}), n is the number of electrons participating in the electrochemical reaction, and Q is the chemical activity of the analytes. In case of physical phenomena, in which apparent redox reactions are not involved, they will generate a potential; however those initial conditions have a non-zero free energy. Therefore, ion concentration gradients across a semipermeable membrane induce a potentiometric response which is the basis of measurements that use ISEs. In pioneering studies by Hyodo et al., they investigated CO, CO_2, and H_2 sensing properties of potentiometric gas sensor by employing noble metals (Ag, Au, Ir, Ru, Rh, Pd, or Pt), loaded metal oxides (Bi_2O_3, CeO_2, In_2O_3, SnO_2, ZnO, or V_2O_5), or carbon black as sensing electrode materials and anion-conducting polymers (ACP) electrolyte in order to improve the selectivity of the resulting chemical sensors [112–117]. The gas sensing mechanism was discussed as the overall potential (sensing electrode potential) arising from the electrochemical reduction of oxygen and CO oxidation balanced with wet synthetic air (57%RH) at 30°C based on the following equations (Eq. (2) and(3)):

$$1/2O_2 + H_2O + 2e^- \rightarrow 2OH^- \tag{2}$$

$$CO + 2OH^- \rightarrow CO_2 + H_2O + 2e^- \tag{3}$$

Among the sensors, Pt-loaded SnO_2 exhibited the most excellent CO selectivity against H_2. On the other hand, Au-loaded In_2O_3 or SnO_2 effectively improved the magnitude of the CO and H_2 responses, resulting in a relatively poor CO selectivity against H_2. However, the selectivity was improved after heat treatment of the Au-loaded In_2O_3 or SnO_2 powder under a reducing atmosphere at 250°C [113, 114]. Based on electrical transduction modes, dynamic processes, such as chemical and diffusion which occurred at the sensor surface under the steady-state condition, result in a thermodynamically accurate signal for potentiometric sensors following Nernst's law of thermodynamics, whereas amperometric sensors relate to Faraday's law (**Table 1**).

3.2 Electrical device sensors

Conductometric gas sensor is an electrical device-based measurement, which measures the signal induced by the change of CP electrical properties as a result

Electrochemical sensor	Sensor signal vs. [gas]	Principle
Amperometric	$E = E_c + k\ln P$	Kinetics (Faraday's law)
Potentiometric	$E = kP$	Thermodynamics (Nernst's law)

Table 1.
Differences between potentiometric and amperometric gas sensor.

of analyte interaction, and no electrochemical reactions take place [100]. Because of their cost-effectiveness and sensitivity, conductometric gas sensors can be used to study the analyte interaction with the sensing materials leading to a resistance change (Eq. (4)). This process causes changes in carrier density or mobility, resulting in a conductivity change (ρ) which is the reciprocal of resistivity (Eq. (5)).

$$\Delta R = \frac{R_o - R_{exposure}}{R_o} \tag{4}$$

$$\rho = \frac{RA}{L} \tag{5}$$

where R_o is the resistance before exposure and R, A, and L are the resistance, sample area, and thickness, respectively. The interaction of CPs with an electron acceptor or donor analyte causes changes in both carrier density and mobility, resulting in an enhanced change in conductivity at the electrode/CP interface, as a result of modulation of the Schottky barrier height (determined by the difference in work function of the intrinsically CP material). When a p-type CP donates electrons to analyte gas molecules, its hole conductivity increases, whereas electron-accepting CPs result in a decrease in conductivity. At the electrode/CP interface, a space charge region is created, and the effective resistance greatly depends on the bias voltage applied during the measurement [118]. Accordingly, there are two different types of conductometric sensor-based CPs.

3.2.1 Polymer-absorption sensors (chemiresistors)

Chemiresistors are the most common type of sensors which can measure the change in the resistance of an electrically active sensitive material on exposure of a target gas analyte or a medium [119]. In addition to their small-sized low-power devices, chemiresistors exhibited good sensitivity and are amenable for online monitoring of various toxic chemicals. Compared with standard electrochemical sensors, chemiresistors do not require liquid electrolyte to work properly. The measured electrical resistance change as the output is attributed to absorption/adsorption of gas analytes into the sensitive material (**Figure 4**). It is a known fact that the conductivity of an identical CP material varies according to the method of preparation and the thickness of the film [120], which has a considerable influence over the surface morphology. In addition, the CP/insulating substrate (oxides such as glass, quartz, sapphire) interface is another aspect which may contribute to the overall conductivity. As a result, the degree of hydration alters the surface conductivity of the substrate because of the interfering water vapors when chemiresistors are operated at room temperature [121]. Making such a substrate surface rather hydrophobic before depositing CP material may mitigate this problem [121].

In the mid-1990s, Agbor et al. demonstrated the deposition of PANI thin films by various techniques (evaporation, spinning, and the Langmuir–Blodgett) as chemiresistor gas sensor of NO_x, H_2S, SO_2, CO, and CH_4 [122]. All types of deposited PANI/EB were sensitive to NO_x, H_2S gas down to 4.0 ppm, whereas only spun

and evaporated PANI/EB dissolved in NMP were responsive to SO_2. Then after, recent studies investigated the design of flexible room temperature chemiresistive NH_3 [123–126], and CO_2 [127] gas sensor based on nanostructured PPY and PANI was synthesized via an in situ chemical polymerization with an aid of dual templates, MO and CTAB. This work represented competitive results for pure, metal-free, and flexible CP sensors operated at room temperature for monitoring NH_3 sensor in workplaces and air pollution with a fast response time and a high selectivity. Bartlett and coworkers have used poly-5-caboxyindole, PPY, and PANI and their derivatives formed by electrochemical polymerization as sensors for alcohols, ether, and other organic vapors; however it showed a low sensitivity [128–130] and an incomplete desorption of the gas molecules [128]. Of the four polymers investigated, poly-5-caboxyindole was the most stable and represented a reproducible behavior. A chemiresistive type H_2 gas sensor based on PANI and PANI/CNT composite at room temperature has been developed by Srivastava et al. [131]. The sensor response showed a higher response after doping of CNT using IDE-type sensor due to a significant interaction between H_2- and CNT-doped PANI composites. In an interesting study by Xue et al., they fabricated a miniaturized chemiresistor gas sensor to next-generation high-performance sensors based on oriented single crystal PPY nanotube (SCPNT) arrays with an ultrathin wall thickness prepared with a combination of cold-wall VDP and template-assisted synthesis using AAO template. A SCPNT chemiresistor sensor exhibited a superior sensing capability to NH_3 gas at a low detection limit down to 0.05 ppb at room temperature, surpassing commercially metal oxide-based sensors [132]. The ultrahigh sensor sensitivity originating from not only higher crystal orientation but also hollow structure and high surface area of the nanotubes allowed the easy diffusion of gas molecules, since the thickness of the SCPNT walls is only about 10 nm scale. An innovative flexible chemiresistor NH_3 gas sensor was fabricated by an in situ chemical oxidative polymerization of PANI with multiwalled CNTs [133] and S, N-doped graphene quantum dots (S, N:GQDs) [134, 135]. A significant increase in the gas sensing performance with improved sensor response/recovery characteristics could be realized at trace-level detection under ambient conditions. The response of S, N:GQDs/PANI composite toward NH_3 gas was five times higher than pure PANI, because the S, N:GQDs cavities facilitated large interaction sites for NH_3 via π-electron networks. Also, the enhancement in PANI/MWCNTs performance was attributed to the physisorption/chemisorption of NH_3 gas due to the synergetic cooperation between acid–base doping/dedoping effect of PANI and the electron transfer between NH_3 molecules and CNT or GQDs. Once NH_3 has adsorbed onto the surface of PANI, it reacted with amine (N-H) groups of PANI forming NH_4^+, resulting in the localization of PANI polarons, and thus increased the sensor resistance.

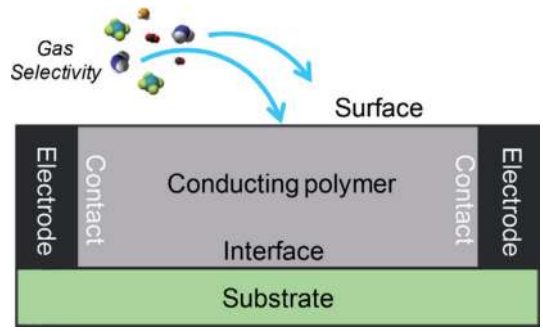

Figure 4.
Schematic illustration of the chemiresistor sensor principle based on chemically sensitive CPs for selective detection of chemical sensing materials.

For maximizing the renewable energy recovery, Xue and coworkers designed a flexible hierarchical PANI/CNT nanocomposite film-based electronic gas sensor for a real-time monitoring of NH_3 in anaerobic digestion from 200 ppb to 50 ppm at room temperature [136]. The sensor exhibited a fast response/recovery time with excellent selectivity to NH_3 compared to other VOCs, such as methanol, ethanol, acetone, dichloromethane, isopropyl alcohol, ethylene glycol, and pyridine due to the high surface area of nanocomposite films. An in situ synthesis of SnO_2-rGO)-PANI (SGP) nanocomposite via surfactant-free precursor at low temperature was investigated for enhanced performance of NH_3 gas sensor [137]. From XPS, the well-defined p-n hetero junction existed in the hybridized SGP nanocomposite dramatically enhanced the sensing activity, selectivity, and chemical stability, in comparison of pure SnO_2 and SnO_2-rGO hybrid. In addition, Ye et al. reported the rGO/Poly (3-hexylthiophene) (rGO/P3HT) composite film prepared by spray process for constructing the resistive NH_3 sensor [138]. The composite film sensor exhibited better sensing properties and reversibility than pure rGO, as a result of π-π interaction between rGO and P3HT. Moreover, Sharma and coworkers demonstrated the synthesis of Al-SnO_2-PANI, MWCNT-PANI, and MWCNT-PEDOT-polystyrene sulfonic acid (PSS) nanofibers via electrospinning technique for H_2 and NH_3 gas sensing application [139, 140]. On exposure to 1000 ppm of H_2 gas, the Al-SnO_2-PANI nanofiber composite showed fast response/recovery at 48°C [139]. MWCNT-PEDOT-PSS was found to be more effective than MWCNT-PANI composite in terms of sensitivity and repeatability for NH_3 gas [140]. However, the sensor presented a major challenge of complete recovery of chemisorbed NH_3 from CNT; the research group proposed a trial experiment for sensor complete recovery within a short time (20 min) using a combination of heat and DC electric field.

Besides, various metals and/or metal oxides were also introduced to further enhance the response/recovery kinetics of the sensing materials. Chemiresistor gas sensing behavior of NH_3 based on nanostructured PPY/SnO_2 [141], PPY/ZnO [142–144], PPY/Zn_2SnO_4 [145], PPY/Ag-TiO_2 [146], PPY/silicon nanowires (PPY/SNWs) [147], PANI/SnO_2 [148], PANI/ZnO [149], PANI/In_2O_3 [150], PANI/TiO_2 [151], PANI/flower-like WO_3 [152], PANI/SnO_2/rGO [153], PANI-TiO_2-Au [154], and Ag-AgCl/PPY [155] has recently been studied so far. The CP/metal oxide nanocomposite thin films exhibited an outstanding response time of 2 S for NH_3 at very low concentration of 50 ppb in air with respect to methanol and ethanol vapors [156]. Thin films of Cu/PANI have also been examined as a sensor toward different gases, such as NH_3, CO, CO_2, NO, and CH_4 at room temperature [157]. Incorporation of Cu nanoparticles improved the response and the recovery times, in addition to its excellent selectivity toward NH_3 due to doping and dedoping processes of PANI. Composite of Pd-PANI-rGO [158] has been recently synthesized to fabricate a highly sensitive and selective chemiresistive H_2 gas sensor. In addition to high surface area of the PANI-GO composite, the fast spillover effect and hydrogen dissociation over Pd significantly enhanced the sensing performance. Other studies by Xu and coworkers employing films of SnO_2-ZnO/PANI [159] and SnO_2/PANI [160] hybrids as NO_2 gas sensors prepared by the solvothermal hot-press (SHP) process were demonstrated. The later sensors exhibited much high affinity and selectivity to a low concentration of NO_2 gas at 140°C caused by the formation of p-n junction. For porous SnO_2-ZnO/PANI, a high selective sensor responded to a low NO_2 concentration at 180°C, due to the porous nature of SnO_2 and high ZnO content (20 wt.%). Mane et al. investigated chemiresistive NO_2 gas sensors based on DBSA-doped PPY/WO_3 and CSA-doped PPY/NiO nanocomposites at room temperature [161, 162]. The sensor can successfully detect NO_2 gas at a concentration as low as 5 ppm. The enhanced gas sensing properties would be assigned to the formation of random nano p-n junctions distributed over the polymer surface film

and activity of dopants. Moreover, Mondal and coworkers [163] reported a green chemical route synthesis of P3TH/CdSe (QDs) nanocomposites as a chemiresistive $CHCl_3$ gas sensor at concentrations range of 100–1200 ppm at room temperature. On illumination of the sensor with a monochromatic light of 600 nm, an enhancement of charge transfer in nanocomposites was photo-induced, resulting in an improvement in sensor response and recovery time.

3.3 Optical device sensors

The gas sensors based on optical transductions are described as change in absorbance and luminescence as a result of gas analytes, interaction with a sensitive material [164]. For signal generation, optical parameters such as refractive index and reflectivity have been used. Optical gas sensors have been recently utilized for multi-analyte array-based gas sensing, due to low cost, miniaturized optoelectronic light sources, and efficient detectors [164]. Based on the signal generated due to intrinsic properties of sensing material, optical sensors are classified as absorption and luminescence.

3.3.1 UV–vis and infrared sensors

The UV–visible and near infrared (NIR) spectra can reflect the electron configurations of CPs. After doping process, the spectral absorbance of CP film is changed with an appearance of new bands due to the formation of polarons and bipolarons [165]. Thus, the interaction of gas analytes at CP film interfaces can be detected by the change in spectra of UV–vis or NIR. When an ultrathin film of CP was deposited on a glass, an optic sensor can be fabricated to record the corresponding spectrum (absorbance or transmittance) by using conventional spectrometers [166]. However, colorimetry is limited in sensitivity to an individual analyte and not useful for in situ applications [167]. For IR sensors, they can only monitor specific analytes of nonlinear molecules; in addition, the measurements are influenced by humidified environment [167]. So far, UV–vis–NIR spectrophotometer has been used to study the sensing characteristics of PANI to a variety of VOCs [168]. Tavoli and Alizadeh designed an optical NH_3 gas sensor based on nanostructure PPY doped with eriochrome cyanine R (ECR) thin film as a dopant for optical selectivity of NH_3 gas using UV–vis spectroscopy with a fast response time (50 s) and a high sensitivity in the concentration range of 15–260 μg L^{-1} [169]. The sensor showed a low detection limit of 5 μg L^{-1} and a good reproducibility.

3.3.2 Fiber-optic devices

Fiber-optic sensors are a class of optical sensors that use optical fibers to detect chemical analytes. Light is generated by a light source and is sent through an optical fiber, then reflects the absorption property of the CP surface when it returns through the optical fiber, and finally is captured by a photo detector [170]. Sensors based on fiber optics used the light guiding properties of the optical fibers to carry the light into and from the CP active layer [171]. However, this type of optical sensor has some drawback concerning the complication of associated electronics and software, cost-effectiveness, concentration limitation, short lifetime due to photobleaching, and limited ability to transmit light through optical fiber over long distances [167, 172]. A fiber-optic device based on PANI was used to detect HCl, NH_3, hydrazine (H_4N_2), and dimethyl methylphosphonate (DMMP, a nerve agent, sarin stimulant) [173]. Muthusamy and coworkers developed gas sensors

based on PPY and PPY/Prussian blue (PPY-PB) nanocomposite coating on fiber optic to monitor NH_3, acetone, and ethanol gases at room temperature [174]. The PPY-PB nanocomposite-based fiber-optic sensor exhibited an enhanced sensitivity for ethanol than pure PPY nanoparticles, and spectral intensity increases linearly with increasing the concentrations of gas. Very recently, Mohammed et al. fabricated an etched-tapered single-mode fiber (SMF) coated with a high surface area PANI/graphite nanofiber (GNF) nanocomposite as optical sensor for NH_3 gas at room temperature in the visible wavelength range [175]. The sensor exhibited a good response time, sensitivity, and reproducibility for NH_3, compared with pure PANI-coated SMF. Furthermore, an optical microfiber sensor was designed by drop coating of PANI doped with dioctyl sodium sulfosuccinate onto a microfiber resonator as a sensor for alcohols [176]. The sensor output spectrum showed red shift in wavelength upon response to various alcohols at different concentrations, due to the increase in dihedral angle and average band gap (lower energy) of PANI fiber. In a recent study by Kim and coworkers reported the application of fiber-optic reflectance sensors (FORS) coated with PPY film for sensing VOCs up to 1 ppm under atmospheric conditions [177]. The variation in the reflected light intensity was caused by the formation of polaron-bipolaron and film swelling when interacted with VOCs.

3.3.3 Surface plasmon resonance (SPR)

Surface plasmon resonance is another class of optical sensors which referred to excitation of surface plasmon-based optical sensor for chemical sensing utilizing light. SPR optical sensor is a thin film refractometer sensing device which measures the changes in refractive index that occurred at the surface of a plasmon-supported metal film. On excitation by the monochromatic light, a change in the refractive index of a dielectric material gives rise to a change in propagation constant of the surface plasmon (prism coupled, i.e., attenuated total reflectance (ATR), waveguide coupled, and grating coupled) [178, 179]. The propagation constant of a radiation alters the characteristics of light wave coupled to the surface plasmon, e.g., coupling angle, coupling wavelength, and intensity phase [180]. After exposing to analytes, the minimum in the reflectance curve can be shifted, indicating the presence of analyte. The sensitivity of this type of sensors is high, but the detecting procedures are complicated. A SPR device was explored by Agbor and coworkers using PANI thin films to detect NO_2 and H_2S gases, resulting in an increase in reflectivity and resonance angle [180].

3.4 Mass-sensitive device sensors

Mass-sensitive devices transform the mass change at a specially modified surface into a change of a property of the piezoelectric material. Surface acoustic wave (SAW) and the quartz crystal microbalance (QCM) techniques are the main categories of piezoelectric gas sensing devices [181]. SAW and QCM are the simplest piezoelectric devices with a selective coating deposited on the surface to serve as an adsorptive surface capable of measuring an extremely small mass change at room temperatures [182]. Interestingly, SAW and QCM sensors are very promising and are widely accepted as smart transducers for their miniaturized design, possibility of wireless integration, high thermal stability, inertness, and room temperature operation. In addition, they can be easily combined with a variety of recognition sensitive layers for sensing applications ranging from small gas molecules to large biomolecules or even whole cell structures.

3.4.1 Surface acoustic wave

Surface acoustic wave resonators represent one of the most prominent acoustic devices for their exceptionally high frequency from several hundred MHz to GHz, which can record remarkably diminutive frequency shifts resulting from exceptionally small mass loadings making them potentially suitable in mass sensing applications [183]. Clearly, SAW resonator is a sensitive layer coated on the gap between a transmitter (an input) and a receptor (an output) interdigital transducers (IDTs) coating on the top of the piezoelectric crystal to design a SAW gas sensor [184]. An input radio-frequency voltage is applied across the transmitter IDTs, inducing deformations in the piezoelectric crystal that give rise to an acoustic wave, traversing the gap between two IDTs. When it reaches the receptor IDTs, the mechanical energy was converted back to radio-frequency voltage. The adsorption/desorption of gas on the CP film on the gap modulates the wave propagation characters, and a frequency shift can be recorded between the input and output voltages. In the sense of applications, a SAW sensor based on fibrous PANI nanocomposites layers prepared by chemical oxidative polymerization of aniline in the presence of finely divided metal oxides deposited on ZnO/64° YX $LiNbO_3$ SAW transducer to detect H_2, NO_2, NO, CO_2 and CO gases [185–188]. The designed SAW sensor exhibited improved sensitivity and repeatability of the gas molecules in ppm level at room temperature. Attractive studies utilized PPY nanocomposite-based SAW gas sensors deposited onto 128° YX-$LiNbO_3$ substrate via Langmuir-Blodgett (LB) method due to high sensitivity and low cost. The LB PPY nanocomposite-based SAW exhibited excellent selectivity toward low NH_3 concentration of 20 ppm, with respect to other interfering gases, such as CO, CH_4, H_2, and O_2, at room ambient temperature [189–191]. By merging with electrical conductivity gas response, the sensing mechanism for gas detection has been investigated as elastic loading. Very recently, SAW integrated with PPY and PPY/TiO_2 films has been utilized for NO_2 and H_2S detection at room temperature by the self-assembly method [192]. Upon exposure to NO_2, the SAW sensors coated with PPY film showed a negative frequency shift (ΔF) tendency, in contrast to PPY/TiO_2 that exhibited a faster sensor response and a higher sensitivity. Besides, the selectivity was greatly improved by addition of TiO_2 to PPY.

3.4.2 Quartz crystal microbalance

The advantage of conceptual simplicity, relative ease of modification, chemical inertness of the substrates, ruggedness, low cost, and ready availability of piezoelectric transducers have encouraged the development of QCM technique in various sensor applications. In addition, the sensitivity of piezoelectric transducers is based on the mass per unit area, suggesting miniaturization without losses in their sensitivity. The associated electronics are fairly simple, and frequency measurements are very precise (<1 part in 10^7) [193]. As illustrated in **Figure 5**, a QCM sensor consists of a quartz disk coated with metal electrodes on both sides (usually Pt or Au). When a voltage is applied to the quartz crystal plate, it can oscillate at a specific frequency, and the relation between frequency change (ΔF) of the oscillating crystal and the mass change (Δm) on the quartz surface was described by Sauerbrey empirical derivation (Eq. (6)) [195]. The change of ΔF (Hz) in the area of the electrode (A cm^{-2}) in terms of the mass increment, Δm (g cm^{-2}), loaded onto the crystal surface under a fundamental resonant frequency F_0 can be estimated from Eq. (1), where N, F_0, ρ, μ, and A are the harmonic overtone, the fundamental resonance frequency, the crystal density (2.649 g cm^{-3}), the elastic modulus of the quartz crystal (2.947×10^{11} g cm^{-1} s^{-2}), and the surface area, respectively.

$$\Delta F = \frac{2NF_0^2}{\sqrt{\rho\mu}}\frac{\Delta m}{A} \quad (6)$$

During the past few decades, the relationship between frequency shift and mass change, which was initially described by Sauerbrey, has been extensively applied for chemical sensing [182]. The ΔF, which is proportional to a mass adsorbed and/or sorbed on sensitive layers of distinct morphologies coated over the QCM electrode, is constantly monitored to identify and quantify the target analyte at the ng level (ng cm^{-2}) [182].

The interaction between target molecules and sensitive coating layers (known as "guest-host interaction") plays an important role in the sensing mechanism. Such a guest-host interaction is considered as an adsorption process involving enrichment of guest species at the interface of a certain adsorbent, such as CP nanomaterials (**Figure 5**). In terms of high sensitivity and selectivity, the fabrication of CP nanomaterials is an important step toward the development of efficient advanced detection sensors. Since 1964, a QCM sensor had been implemented by King into a gas chromatography system for the detection of hydrocarbons [196]. Then after, QCM sensor device has been successfully applied as a sensitive tool to sense mass interfacial [197] and polymer film properties [198–201]. Accordingly, ΔF was investigated in terms of rigid mass changes, based on the Sauerbrey equation. The QCM technique has been used in the fields of gas sensing application including gas mixture analysis [202], discrimination of aromatic optical isomers [203], and VOC vapors detection [204, 205]. In the early trials, Gomes et al. [206] have used uncoated quartz crystals with gold electrodes to detect and quantify volatile amines, such as *iso*-propylamine, *n*-butylamine, *s*-butylamine, and *tert*-butylamine; however this method suffers from low sensitivity. Attention has been paid to the development of efficient QCM sensors which rely greatly on the utilization of CPs as sensitive coatings. Thin film-coated QCM sensors were pioneered by Ayad et al. [207–212]. For example, a QCM technique concomitant with sensitive layers of CPs, PANI in the form of ES, and EB prepared by the in situ chemical oxidative polymerization was explored to detect and quantify varieties of VOCs in air, such as chlorinated aliphatic hydrocarbons, like CCl_4, $CHCl_3$, CH_2Cl_2, and $ClCH_2$-CH_2Cl; aliphatic alcohols, like CH_3OH, C_2H_5OH, C_3H_7OH, and C_4H_9OH; and aliphatic amines including CH_3NH_2, $(CH_3)NH$, $(CH_3)_3N$, and $(CH_3CH_2)_3N$ [213–217]. The adsorption mechanism was discussed as a kind hydrogen bonding or a dipole/dipole interaction formed between the imine and amine sites of PANI with chemical vapor. The difference in adsorption affinity was attributed to the differences in their chemical structure and strength of the electrostatic interactions. Interestingly, the PANI adsorption kinetics (Eq. (7)) [217] and diffusion of chemical vapor were carefully discussed, in terms of diffusion coefficient (D) using Fick's second equation (Eq. (8)), which has been reviewed by Crank [218].

$$\frac{\Delta F_t}{\Delta F_\infty} = 1 - e^{-kt} \quad (7)$$

$$\frac{\Delta F_t}{\Delta F_\infty} = 4\sqrt{\frac{D}{\pi}}\frac{t^{1/2}}{L} \quad (8)$$

$$\Delta F_t = F_{polymer} - F_t \text{ and } \Delta F_\infty = F_{polymer} - F_\infty \quad (9)$$

where k is the pseudo-first-order rate constant for vapor uptake. ΔF_t and ΔF_∞ (Hz) are the frequency changes due to the adsorption uptake of the vapor into the polymer film at any time t and at the steady-state, respectively. $F_{polymer}$ is the

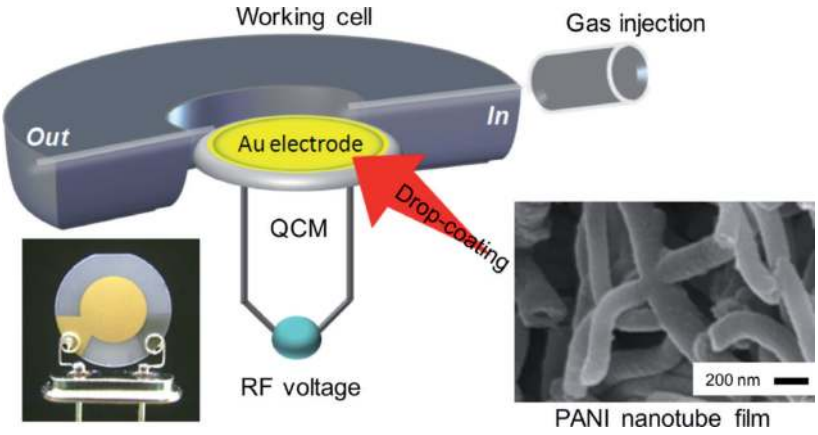

Figure 5.
Schematic representation of the interaction of an analyte with PANI nanotube prepared with CSA coating on a QCM (modified and adapted with permission from Ref. [194]. Copyright 2014, Wiley-VCH Verlag GmbH &Co. KGaA, Weinheim).

frequency of the polymer film estimated from QCM. L (cm) is the film thickness and can be determined by the density of the polymer and mass change, and Δm (g cm^{-2}) is from the Sauerbrey equation (Eq. (4)). The k and D can be calculated from the slope of linear graphs of $\ln(1 - \Delta F_t/\Delta F_\infty)$ against t and $\Delta F_t/\Delta F_\infty$ as a function of $t^{1/2}/L$, respectively.

Li et al. constructed a sensor using water-soluble PANI and PANI-TiO_2 nanocomposite-coated QCM for a selective detection of amine vapors [219, 220]. The nanocomposite exhibited a higher sensing affinity and good selectivity toward $(CH_3)_3N$ and $(CH_3CH_2)_3N$ than other VOCs, such as C_2H_5OH, CH_3-COO-CH_2-CH_3, CH_2O, and CH_3CHO. As the van der Waals absorption is the main interaction between PANI and amine, the sensor responses could be completely recovered after purging N_2 at room temperature. Further, PANI/ES films doped with several dopants, such as HCl and DBSA, and 1,5-naphtalenedisulfonic acid (1,5-NDSA))-coated QCM sensor films have been fabricated to detect BTEX vapors [221]. The ΔF due to adsorption of VOCs is attributed to electrostatic interactions between vapor molecules and dopant in PANI/ES films. Interestingly, PANI-DBSA films were found to be highly sensitive and selective to *p*-xylene compared with toluene and benzene. Further, the adsorption behavior of poly(3-butoxythiophene) (P3BOT) mixed with stearic acid (SA) LB film-coated QCM was studied as a sensing material for series of chemical vapor analytes, such as chlorinated aliphatic hydrocarbons and some short-chain aliphatic alcohols [222]. On exposure to vapor analyte, the frequency of the QCM was changed, due to the dipole/dipole or hydrogen bonding interaction with P3BOT/SA film. Additionally, a control of sensitivity and selectivity of the sensor could be achieved through polymer functionalization with ether group, difference in molecular weight, and structure of the chemical vapors.

Gas sensing properties of the CPs have dramatically improved after incorporation of other nanomaterials such as CNTs, GO, metals, and other nanometal oxides. Very recently, Wang et al. fabricated a gas sensor by using PPY and PPY/TiO_2 coating on QCM electrode for detecting different chemical vapors [223]. As a result, the sensor coated with PPY/TiO_2 was found to exhibit a better sensing performance, long-term stability, and excellent reversibility, as well as acceptable selectivity toward NH_3 in comparison to $(CH_3)_3N$, H_2S, and C_2H_5OH. Based on QCM measurements, researchers could fabricate a PPY/TiO_2 sensor for evaluating shelf-life quality changes of three typical foodstuffs (mango, egg, and fish) during 1-week storage.

Novel low-humidity sensors were investigated by the in situ photopolymerization of PPY/Ag/TiO_2 nanoparticle composite thin film coating on QCM [224]. Room temperature highly sensitive sensors with short response/recovery time for humidity based on GO/SnO_2/PANI and PANI-GO coating on QCM were explored by Zhang et al. [225, 226]. The adsorption process of water molecules on QCM senor was carefully discussed using Langmuir adsorption isotherm model.

3.5 Summary and perspectives

With the development of nanotechnology, CP nanostructures integrated into advanced electronics have pursuit of better sensing systems during the past decade for fabricating miniaturizing state-of-the-art sensor devices, due to their continuously discovered unique chemical and physical characteristics, such as reversible signal transduction processes, low operating temperature, tunable sensitivity, and design flexibility. However, sensing technologies based on CPs still require significant incubation and device development. From the viewpoint of sensing activity, control over CP characteristics is necessary to improve sensitivity, selectivity, and stability to design advanced detection sensors. The desired set of physicochemical properties can be introduced into the CPs through the rational molecular design of specific receptors or judicious functionalization of the CP surface with a molecular recognition, leading to enhanced specificity via covalent attachments and reproducibility in response. Also, for large-scale synthesis, it is important to develop reliable routes to synthesize CP nanostructures and nanocomposites with controlled morphology. Of the exciting synthetic methods, the soft template approach is somewhat advantageous in both large-scale synthesis and size/shape control. Such improvements in their molecular structure and crystallinity and an increase in conjugation length are crucial for increasing room temperature conductivity. Another concern is that CPs are also susceptible to environmental perturbations such as moisture, heat, and light, which may degrade over time, even in dry, oxygen-free environments, and thus much attention must be paid to improving their long-term stability that is considered to be an important factor in pursuing high sensor reliability for an ever-increasing role in online environmental monitoring, industrial safety control, and security. Since the fabrication of nanostructured CPs, response time and sensitivity have experienced impressive improvements with great advances in sensor nanotechnology. However, selectivity is still a challenging task for detecting specific target analyte in a multi-analyte environment which hindered the widespread application of CP-based sensors. Besides, the demand for miniaturization has encouraged for designing portable sensor devices, lower power dissipation, and better device integration. In this sense, nanostructured CPs have considerable potential for fabricating miniaturized multi-sensing arrays by using microcontact printing, surface-directed assembly, site-specific polymerization, inkjet printing, etc. Interestingly, CPs are highly compatible with a flexible substrate, which opens up the possibility of realizing all-polymer electronics. From viewpoint, we believe that nanostructured CPs still have many unexplored potentials and will definitely play an expanding role in future sensor technology for exclusively designing of next-generation sensors involving high sensitivity, high reliability, multi-analyte determination, miniaturization, and structural flexibility due to their fascinating chemical/physical properties that are not available in other materials. Thus, it is anticipated that extensive future research studies into the development of flexible high-performance sensors by utilizing CPs will be expected in the near future.

DOI: http://dx.doi.org/10.5772/intechopen.89888

Author details

Nagy L. Torad[1] and Mohamad M. Ayad[1,2]*

1 Chemistry Department, Faculty of Science, University of Tanta, Tanta, Egypt

2 Institute of Basic and Applied Sciences, Egypt-Japan University of Science and Technology (E-JUST), New Borg El-Arab City, Alexandria, Egypt

*Address all correspondence to: mohamad.ayad@ejust.edu.eg
and mohamed.ayad@science.tanta.edu.eg

IntechOpen

References

[1] Shirakawa H, Louis EJ, MacDiarmid AG, Chiang CK, Heeger AJ. Synthesis of electrically conducting organic polymers: Halogen derivatives of polyacetylene, (CH)x. Journal of the Chemical Society, Chemical Communications. 1977:579-580

[2] Chiang CK, Fischer CR, Park YW, Heeger AJ, Shirakawa H, Louis EJ, et al. Electrical conductivity in doped polyacetylene. Physical Review Letters. 1977;**39**:1098-1101

[3] Chiang CK, Druy MA, Gau SC, Heeger AJ, Louis EJ, MacDiarmid AG, et al. Synthesis of highly conducting films of derivatives of polyacetylene, (CH)x. American Chemical Society. 1987;**100**:1013-1015

[4] DelamarM,LacazePC,DumousseauJS, Dubois JE. Electrochemical oxidation of benzene and biphenyl in liquid sulfur dioxide: Formation of conductive deposits. Electrochimica Acta. 1982;**27**:61-65

[5] Diaz AF, Kanazawa KK, Gardini GP. Electrochemical polymerization of pyrrole. Journal of the Chemical Society, Chemical Communications. 1979:635-636

[6] Waltman RJ, Bargon J, Diaz AF. Electrochemical studies of some conducting polythiophene films. The Journal of Physical Chemistry. 1983;**87**:1459-1463

[7] Diaz AF, Logan JA. Electroactive polyaniline films. Journal of Electroanalytical Chemistry. 1980;**111**:111-114

[8] MacDiarmid AG. Synthetic metals: A novel role for organic polymers. Synthetic Metals. 2001;**125**:11-22

[9] Ibanez JG, Rinćon ME, Gutierrez-Granados S, Chahma M, Jaramillo-Quintero OA, Frontana-Uribe BA. Conducting polymers in the fields of energy, environmental remediation, and chemical-chiral sensors. Chemical Reviews. 2018;**118**:4731-4816

[10] Jang J. Conducting polymer nanomaterials and their applications. Advances in Polymer Science. 2006;**199**:189-260

[11] Yoon H, Jang J. Conducting-polymer nanomaterials for high performance sensor applications: Issues and challenges. Advanced Functional Materials. 2009;**19**:1567-1576

[12] Janata J, Josowicz M. Conducting polymers in electronic chemical sensors. Nature Materials. 2003;**2**:19

[13] Li C, Bai H, Shi G. Conducting polymer nanomaterials: Electrosynthesis and applications. Chemical Society Reviews. 2009;**38**:2397-2409

[14] Kwon OS, Song HS, Park TH, Jang J. Conducting nanomaterial sensor using natural receptors. Chemical Reviews. 2019;**119**:36-93

[15] Li D, Huang J, Kaner RB. Polyaniline nanofibers: A unique polymer nanostructure for versatile applications. Accounts of Chemical Research. 2008;**42**:135-145

[16] Kaushik A, Kumar R, Arya SK, Nair M, Malhotra BD, Bhansali S. Organic-inorganic hybrid nanocomposite-based gas sensors for environmental monitoring. Chemical Reviews. 2015;**115**:4571-4606

[17] Hatchett DW, Josowicz M. Composites of intrinsically conducting polymers as sensing Nanomaterials. Chemical Reviews. 2008;**108**:746-769

[18] Ćiric-Marjanović G. Recent advances in polyaniline research:

Polymerization mechanisms, structural aspects, properties and applications. Synthetic Metals. 2013;**177**:1-47

[19] Ayad MM, Zaki EA. Synthesis and characterization of polyaniline films using Fenton reagent. Journal of Applied Polymer Science. 2008;**110**:3410-3419

[20] Xia Y, Wiesinger J, MacDiarmid AG, Epstein AJ. Camphorsulfonic acid fully doped polyaniline emeraldine salt: Conformations in different solvents studied by an ultraviolet/visible/near-infrared spectroscopic method. Chemistry of Materials. 1995;**7**:443-445

[21] Baker CO, Huang X, Nelson W, Kaner RB. Polyaniline nanofibers: Broadening applications for conducting polymers. Chemical Society Reviews. 2017;**46**:1510-1525

[22] Sen T, Mishra S, Shimpi NG. Synthesis and sensing applications of polyaniline nanocomposites: A review. RSC Advances. 2016;**6**:42196-42222

[23] Ayad MM, Amer WA, Zaghlol S, Minisy IM, Bober P, Stejskal J. Polypyrrole-coated cotton textile as adsorbent of methylene blue dye. Chemical Papers. 2018;**72**:1605-1618

[24] Ayad MM, Amer WA, Zaghlol S, Maráková N, Stejskal J. Polypyrrole-coated cotton fabric decorated with silver nanoparticles for the catalytic removal of *p*-nitrophenol from water. Cellulose. 2018;**25**:7393-7407

[25] Ayad MM, Zaghlol S. Nanostructured crosslinked polyaniline with high surface area: Synthesis, characterization and adsorption for organic dye. Chemical Engineering Journal. 2012;**204-206**:79-86

[26] Stejskal J, Sapurina I, Trchova M. Polyaniline nanostructureś and the role of aniline oligomers in their formation. Progress in Polymer Science. 2010;**35**:1420-1481

[27] Ayad MM, Salahuddin NA, Fayed A, Bastakoti BP, Suzuki N, Yamauchi Y. Chemical design of a smart chitosan-polypyrrole-magnetite nanocomposite toward efficient water treatment. Physical Chemistry Chemical Physics. 2014;**16**:21812-21819

[28] Ayda MM, Amer WA, Kotp MG, Minisy IM, Rehaba AF, Kopecký D, et al. Synthesis of silver-anchored polyaniline–chitosan magnetic nanocomposite: A smart system for catalysis. RSC Advances. 2017;**7**:18553-18560

[29] Ayad MM, Amer WA, Kotp MG. Magnetic polyaniline-chitosan nanocomposite decorated with palladium nanoparticles for enhanced catalytic reduction of 4-nitrophenol. Molecular Catalysis. 2017;**439**:72-80

[30] Minisy IM, Salahuddin NA, Ayad MM. Chitosan/polyaniline hybrid for the removal of cationic and anionic dyes from aqueous solutions. Journal of Applied Polymer Science. 2019;**136**:47056. DOI: 10.1002/APP.47056

[31] Amer WA, Al-saida B, Ayad MM. Rational design of a polypyrrole-based competent bifunctional magnetic nanocatalyst. RSC Advances. 2019;**9**:18245-18255

[32] Virji S, Huang J, Kaner RB, Weiller BH. Polyaniline nanofiber gas sensors: Examination of response mechanisms. Nano Letters. 2004;**4**:491-496

[33] Zhang L, Wan M. Self-assembly of polyaniline-from nanotubes to hollow microspheres. Advanced Functional Materials. 2003;**13**:815-820

[34] Trchová M, Šeděnková I, Konyushenko EN, Stejskal J, Holler P,

Ćirić-Marjanović G. Evolution of polyaniline nanotubes: The oxidation of aniline in water. The Journal of Physical Chemistry. B. 2006;**110**:9461-9468

[35] Janošević A, Ćirić-Marjanović G, Marjanović B, Holler P, Trchová M, Stejskal J. Synthesis and characterization of conducting′ polyaniline 5-sulfosalicylate nanotubes. Nanotechnology. 2008;**19**:135606

[36] Ćiric-Marjanović G, Trchová M, Stejskal J. The chemical oxidative polymerization of aniline in water: Raman spectroscopy. Journal of Raman Specroscopy. 2008;**39**:1375-1387

[37] Ayad MM, Prastomo N, Matsuda A. Synthesis and characterization of polyaniline-camphorsulphonic acid nanotube film. Materials Letters. 2010;**64**:379-382

[38] Ayad MM, Prastomo N, Matsuda A, Stejskal J. Sensing of silver ions by nanotubular polyaniline film deposited on quartz-crystal in a microbalance. Synthetic Metals. 2010;**160**:42-46

[39] Prastomo N, Ayad MM, Kawamura G, Matsuda A. Synthesis and characterization of polyaniline nanofiber/TiO_2 nanoparticles hybrids. Journal of the Ceramic Society of Japan. 2011;**119**:342-345

[40] Wang G, Morrin A, Li M, Liu N, Luo X. Nanomaterial-doped conducting polymers for electrochemical sensors and biosensors. Journal of Materials Chemistry B. 2018;**6**:4173-4190

[41] Moozarm P, Woi N, Meng P, Alias Y. Hydrogen peroxide sensor: Uniformly decorated silver nanoparticles on polypyrrole for wide detection range. Applied Surface Science. 2015;**357**:1565-1572

[42] Ghanbari K. Fabrication of silver nanoparticles-polypyrrole composite modified electrode for electrocatalytic oxidation of hydrazine. Synthetic Metals. 2014;**195**:234-240

[43] Yoon H. Current trends in sensors based on conducting polymer nanomaterials. Nanomaterials. 2013;**3**:524-549

[44] Jackowska K, Biegunski AT, Tagowska M. Hard template synthesis of conducting polymers: A route to achieve nanostructures. Journal of Solid State Electrochemistry. 2008;**12**:437-443

[45] Zhang F, Nyberg T, Inganas O. Conducting polymer nanowires and nanodots made with soft lithography. Nano Letters. 2002;**2**:1373-1377

[46] Wu Q-F, He K-X, Mi H-Y, Zhang X-G. Electrochemical capacitance of polypyrrole nanowire prepared by using cetyltrimethylammonium bromide (CTAB) as soft template. Materials Chemistry and Physics. 2007;**101**:367-371

[47] Huang J, Kaner RB. Nanofiber formation in the chemical polymerization of aniline: A mechanistic study. Angewandte Chemie. 2004;**116**:5941-5945

[48] Jang J, Oh JH, Stucky GD. Fabrication of ultrafine conducting polymer and graphite nanoparticles. Angewandte Chemie, International Edition. 2002;**41**:4016-4019

[49] Martin J, Maiz J, Sacristan J, Mijangos C. Tailored polymer-based nanorods and nanotubes by "template synthesis": From preparation to applications. Polymer. 2012;**53**:1149-1166

[50] Zhang F, Liu X, Pan C, Zhu J. Nano-porous anodic aluminium oxide membranes with 6-19 nm pore diameters formed by a low-potential anodizing process. Nanotechnology. 2007;**18**:345302

[51] Xiong S, Wang Q, Xia H. Preparation of polyaniline nanotubes array based on anodic aluminum oxide template. Materials Research Bulletin. 2004;**39**:1569-1580

[52] Jang J, Ko S, Kim Y. Advanced Functional Materials. 2006;**16**:754-759

[53] Jang J, Oh J. A facile synthesis of polypyrrole nanotubes using a template mediated vapor deposition polymerization and the conversion to carbon nanotubes. Chemical Communications. 2004:882-883

[54] Park E, Kwon OS, Park SJ, Lee JS, You S, Jang J. One-pot synthesis of silver nanoparticles decorated poly (3, 4-ethylenedioxythiophene) nanotubes for chemical sensor application. Journal of Materials Chemistry. 2012;**22**:1521-1526

[55] Greiner A, Wendorff JH. Electrospinning: A fascinating method for the preparation of ultrathin fibres. Angewandte Chemie, International Edition. 2007;**46**:5670-5703

[56] Kwon OS, Park SJ, Park HW, Kim T, Kang M, Jang J, et al. Kinetically controlled formation of multidimensional poly (3,4-ethylenedioxythiophene) nanostructures in vapor-deposition polymerization. Chemistry of Materials. 2012;**24**:4088-4092

[57] Guo Y, Tang Q, Liu H, Zhang Y, Li Y, Hu W, et al. Light-controlled organic/inorganic P-N junction nanowires. Journal of the American Chemical Society. 2008;**130**:9198-9199

[58] Gence L, Faniel S, Gustin C, Melinte S, Bayot V, Callegari V, et al. Structural and electrical characterization of hybrid metal-polypyrrole nanowires. Physical Review B: Condensed Matter and Materials Physics. 2007;**76**:115415

[59] Liu R, Lee SB. MnO_2/poly(3,4-ethylenedioxythiophene) coaxial nanowires by one-step coelectrodeposition for electrochemical energy storage. Journal of the American Chemical Society. 2008;**130**:2942-2943

[60] Salabat A, Mirhoseini F, Arjomandzadegan M, Jiryaei E. A novel methodology for fabrication of Ag-polypyrrole core-shell nanosphere using microemulsion system and evaluation of its antibacterial application. New Journal of Chemistry. 2017;**41**:12892-12900

[61] Huang L, Wang Z, Wang H, Cheng X, Mitra A, Yan Y. Polyaniline nanowires by electropolymerization from liquid crystalline phases. Journal of Materials Chemistry. 2002;**12**:388-391

[62] Choi SJ, Park SM. Electrochemical growth of nanosized conducting polymer wires on gold using molecular templates. Advanced Materials. 2000;**12**:1547-1549

[63] Yoon H, Chang M, Jang J. Formation of 1D poly(3,4-ethylenedioxythiophene) nanomaterials in reverse microemulsions and their application to chemical sensors. Advanced Functional Materials. 2007;**17**:431-436

[64] Jang J, Yoon H. Multigram-scale fabrication of monodisperse conducting polymer and magnetic carbon nanoparticles. Small. 2005;**1**:1195-1199

[65] Jang J, Yoon H. Facile fabrication of polypyrrole nanotubes using reverse microemulsion polymerization. Chemical Communications. 2003:720-721

[66] Jang J, Yoon H. Formation mechanism of conducting polypyrrole nanotubes in reverse micelle systems. Langmuir. 2005;**21**:11484-11489

[67] Hong JY, Yoon H, Jang J. Kinetic study of the formation of polypyrrole

nanoparticles in water-soluble polymer/metal cation systems: A light-scattering analysis. Small. 2010;**6**:679-686

[68] Zhong WB, Deng JY, Yang YS, Yang WT. Synthesis of large-area three-dimensional polyaniline nanowire networks using a "soft template". Macromolecular Rapid Communications. 2005;**26**:395-400

[69] Liu Z, Zhang XY, Poyraz S, Surwade SP, Manohar SK. Oxidative template for conducting polymer nanoclips. Journal of the American Chemical Society. 2010;**132**:13158-13159

[70] Zhao B, Nan Z. Formation of self-assembled nanofiber-like Ag@ PPy core/shell structures induced by SDBS. Materials Science and Engineering C. 2012;**32**:1971-1975

[71] Li Y, Bober P, Trchová M, Stejskal J. Polypyrrole prepared in the presence of methyl orange and ethyl orange: Nanotubes versus globules in conductivity enhancement. Journal of Materials Chemistry C. 2017;**5**:4236-4245

[72] Bober P, Stejskal J, Šeděnková I, Trchová M, Martinková L, Marek J. The deposition of globular polypyrrole and polypyrrole nanotubes on cotton textile. Applied Surface Science. 2015;**356**:737-741

[73] Kopecká J, Kopecký D, Vrňata M, Fitl P, Stejskal J, Trchová M, et al. Polypyrrole nanotubes: Mechanism of formation. RSC Advances. 2014;**4**:1551-1558

[74] Varga M, Kopecká J, Morávková Z, Křivka I, Trchová M, Stejskal J, et al. Effect of oxidant on electronic transport in polypyrrole nanotubes synthesized in the presence of methyl orange. Journal of Polymer Science Part B: Polymer Physics. 2015;**53**:1147-1159

[75] Škodová J, Kopecký D, Vrňata M, Varga M, Prokeš J, Cieslar M, et al. Polypyrrole-silver composites prepared by the reduction of silver ions with polypyrrole nanotubes. Polymer Chemistry. 2013;**4**:3610-3616

[76] Stejskal J, Trchová M, Bober P, Morávková Z, Kopecký D, Vrňata M, et al. Polypyrrole salts and bases: Superior conductivity of nanotubes and their stability towards the loss of conductivity by deprotonation. RSC Advances. 2016;**6**:88382-88391

[77] Humpolíček P, Radaszkiewicz KA, Capáková Z, Pacherník J, Bober P, Kašpárková V, et al. Polyaniline cryogels: Biocompatibility of novel conducting macroporous material. Scientific Reports. 2018;**8**:135. DOI: 10.1038/s41598-017-18290-1

[78] Li Y, Bober P, Apaydin DH, Syrový T, Sariciftci NS, Hromádková J, et al. Colloids of polypyrrole nanotubes/nanorods: A promising conducting ink. Synthetic Metals. 2016;**221**:67-74

[79] Dai T, Lu Y. Water-soluble methyl orange fibrils as versatile templates for the fabrication of Conducting polymer microtubules. Macromolecular Rapid Communications. 2007;**28**:629-633

[80] Stejskal J, Sapurina I, Trchová M, Konyushenko EN, Holler P. The genesis of polyaniline nanotubes. Polymer. 2006;**47**:8253-8262

[81] Upadhyay J, Kumar A. Structural, thermal and dielectric studies of polypyrrole nanotubes synthesized by reactive self-degrade template method. Materials Science and Engineering B. 2013;**178**:982-989

[82] Upadhyay J, Kumar A. Investigation of structural, thermal and dielectric properties of polypyrrole nanotubes tailoring with silver nanoparticles.

Composites Science and Technology. 2014;**97**:55-62

[83] Zhang Q, Liu F, Li L, Pan G, Shang S. Magnetic ionic liquid-assisted synthesis of polyaniline/AgCl nanocomposites by interface polymerization. Journal of Nanoparticle Research. 2011;**13**:415-421

[84] Oliveira LVF, Camilo FF. Facile synthesis of silver-polypyrrole nanocomposites: Use of ionic liquid as solvent and template. Synthetic Metals. 2019;**247**:219-227

[85] Lee KJ, Min SH, Oh H, Jang J. Fabrication of polymer nanotubes containing nanoparticles and inside functionalization. Chemical Communications. 2011;**47**:9447-9449

[86] Huang J, Virji S, Weiller BH, Kaner RB. Polyaniline nanofibers: Facile synthesis and chemical sensors. Journal of the American Chemical Society. 2003;**125**:314-315

[87] Tran HD, D'Arcy JM, Wang Y, Beltramo PJ, Strong VA, Kaner RB. The oxidation of aniline to produce "polyaniline": A process yielding many different nanoscale structures. Journal of Materials Chemistry. 2011;**21**:3534-3550

[88] Ding H, Shen J, Wan M, Chen Z. Formation mechanism of polyaniline nanotubes by a simplified template-free method. Macromolecular Chemistry and Physics. 2008;**209**:864-871

[89] Martin CR. Nanomaterials: A membrane-based synthetic approach. Science. 1994;**266**:1961-1966

[90] Wan M. A template-free method towards conducting polymer nanostructures. Advanced Materials. 2008;**20**:2926-2932

[91] Wan M, Huang J, Shen Y. Microtubes of conducting polymers. Synthetic Metals. 1999;**101**:708-711

[92] Tang Q, Wu J, Sun X, Li Q, Lin J. Shape and size control of oriented polyaniline microstructure by a self-assembly method. Langmuir. 2009;**25**:5253-5257

[93] Liu H, Kameoka J, Czaplewski DA, Craighead H. Polymeric nanowire chemical sensor. Nano Letters. 2004;**4**:671-675

[94] Du JM, Zhang JL, Han BX, Liu ZM, Wan MX. Polyaniline microtubes synthesized via supercritical CO_2 and aqueous interfacial polymerization. Synthetic Metals. 2005;**155**:523-526

[95] Wan MX. Some issues related to polyaniline micro—/ nanostructures. Macromolecular Rapid Communications. 2009;**30**:963-975

[96] Zhang LJ, Wan MX. Chiral polyaniline nanotubes synthesized via a self-assembly process. Thin Solid Films. 2005;**477**:24-31

[97] Wang J, Chan S, Carlson RR, Luo Y, Ge GL, Ries RS, et al. Electrochemically fabricated polyaniline nanoframework electrode junctions that function as resistive sensors. Nano Letters. 2004;**4**:1693-1697

[98] Alam MM, Wang J, Guo YY, Lee SP, Tseng HR. Electrolyte-gated transistors based on conducting polymer nanowire junction arrays. The Journal of Physical Chemistry. B. 2005;**109**:12777-12784

[99] Chang M, Kim T, Park HW, Kang M, Reichmanis E, Yoon H. Imparting chemical stability in nanoparticulate silver via a conjugated polymer casing approach. ACS Applied Materials & Interfaces. 2012;**4**:4357-4365

[100] Adam H, Stanisław G, Folke I. Chemical sensors definitions and classification. Pure and Applied Chemistry. 1991;**63**:1274-1250

[101] Tierney MJ, Kim HOL. Electrochemical gas sensor with extremely fast response times. Analytical Chemistry. 1993;**65**:3435-3440

[102] Stetter JR, Li J. Amperometric gas sensors–A review. Chemical Reviews. 2008;**108**:352-366

[103] Rahman MA, Kumar P, Park D-S, Shim Y-B. Electrochemical sensors based on organic conjugated polymers. Sensors. 2008;**8**:118-141

[104] Do J-S, Chang W-B. Amperometric nitrogen dioxide gas sensor: Preparation of PAn/Au/SPE and sensing behavior. Sensors and Actuators B: Chemical. 2001;**72**:101-107

[105] Do J-S, Shieh R-Y. Electrochemical nitrogen dioxide gas sensor based on solid polymeric electrolyte. Sensors and Actuators B: Chemical. 1996;**37**:19-26

[106] Do J-S, Chang W-B. Amperometric nitrogen dioxide gas sensor based on PAn/Au/Nafion®prepared by constant current and cyclic voltammetry methods. Sensors and Actuators B: Chemical. 2004;**101**:97-106

[107] Morrin A, Smyth M, Killard AJ, Ngamna O, Wallace GG, Moulton SE, CrowleyK.SensorComprisingConducting Polymer Materials, European Patent Office. 2007. EP2004840A1

[108] Tiwari A, Gong S. Electrochemical synthesis of chitosan-copolyaniline/ WO3. nH_2O composite electrode for amperometric detection of NO_2 gas. Electroanalysis. 2008;**20**:1775-1781

[109] Do J-S, Chen Y-Y, Tsai M-L. Planar solid-state amperometric hydrogen gas sensor based on Nafion®/ Pt/nano-structured polyaniline/ Au/Al_2O_3 electrode. International Journal of Hydrogen Energy. 2018;**43**:14848-14858

[110] Santos MC, Hamdan OHC, Valverde SA, Guerra EM, Bianchi RF. Synthesis and characterization of V_2O_5/ PANI thin films for application in amperometric ammonia gas sensors. Organic Electronics. 2019;**65**:116-120

[111] Bakker E, Telting-Diaz M. Electrochemical sensors. Analytical Chemistry. 2002;**74**:2781-2800

[112] Hyodo T, Ishibashi C, Yanagi H, Kaneyasu K, Shimizu Y. Potentiometric hydrogen sensors using an anion-conducting polymer as an electrolyte. Reports of the Faculty of Engineering, Nagasaki University. 2012;**42**:42-47

[113] Hyodo T, Takamori M, Goto T, Ueda T, Shimizu Y. Potentiometric CO sensors using anion-conducting polymer electrolyte: Effects of the kinds of noble metal-loaded metal oxides as sensing-electrode materials on CO-sensing properties. Sensors and Actuators B: Chemical. 2019;**287**:42-52

[114] Hyodo T, Goto T, Ueda T, Kaneyasu K, Shimizu Y. Potentiometric carbon monoxide sensors using an anion-conducting polymer electrolyte and Au-loaded SnO_2 electrodes. Journal of the Electrochemical Society. 2016;**163**:B300-B308

[115] Goto T, Hyodo T, Ueda T, Kamada K, Kaneyasu K, Shimizu Y. CO-sensing properties of potentiometric gas sensors using an anion-conducting polymer electrolyte and Au-loaded metal oxide electrodes. Electrochimica Acta. 2015;**166**:232-243

[116] Hyodo T, Ishibashi C, Matsuo K, Kaneyasu K, Yanagi H, Shimizu Y. CO and CO_2 sensing properties of electrochemical gas sensors using an anion-conducting polymer as an electrolyte. Electrochimica Acta. 2012;**82**:19-25

[117] Goto T, Hyodo T, Kaneyasu K, Yanagi H, Shimizu Y. CO sensing properties of electrochemical gas sensors using an anion-conducting polymer as an electrolyte. ECS Transactions. 2013;**50**:267-272

[118] Hagleitner C, Hierlemann A, Lange D, Kummer A, Kerness N, Brand O, et al. Smart single-chip gas sensor microsystem. Nature. 2001;**414**:293-296

[119] Langea U, Mirsky VM. Chemiresistors based on conducting polymers: A review on measurement techniques. Analytica Chimica Acta. 2011;**687**:105-113

[120] Stussi E, Stella R, De Rossi D. Chemoresistive conducting polymer-based odour sensors: Influence of thickness changes on their sensing properties. Sensors and Actuators B: Chemical. 1997;**43**:180-185

[121] Wang PC, Huang Z, MacDiarmid AG. Critical dependency of the conductivity of polypyrrole and polyaniline films on the hydrophobicity/hydrophilicity of the substrate surface. Synthetic Metals. 1999;**101**:852-853

[122] Agbor NE, Petty MC, Monkman AP. Polyaniline thin films for gas sensing. Sensors and Actuators B: Chemical. 1995;**28**:173-179

[123] Syrový T, Kuberský P, Sapurina I, Pretl S, Bober P, Syrová L, et al. Gravure-printed ammonia sensor based on organic polyaniline colloids. Sensors and Actuators B: Chemical. 2016;**225**:510-516

[124] Rawal I, Kaur A. Synthesis of mesoporous polypyrrole nanowires/nanoparticles for ammonia gas sensing application. Sensors and Actuators A. 2013;**203**:92-102

[125] Patois T, Sanchez J-B, Berger F, Rauch J-Y, Fievet P, Lakard B. Ammonia gas sensors based on polypyrrole films: Influence of electrodeposition parameters. Sensors and Actuators B: Chemical. 2012;**171-172**:431-439

[126] Joshi A, Gangal SA, Gupta SK. Ammonia sensing properties of polypyrrole thin films at room temperature. Sensors and Actuators B: Chemical. 2011;**156**:938-942

[127] Chena X, Wong CKY, Yuan CA, Zhang G. Impact of the functional group on the working range of polyaniline as carbon dioxide sensors. Sensors and Actuators B: Chemical. 2012;**175**:15-21

[128] Bartlett PN, Ling-Chung SK. Conducting polymer gas sensors part III: Results for four different polymers and five different vapours. Sensors and Actuators. 1989;**20**:287-292

[129] Bartlett PN, Archer P, Ling-Chung SK. Conducting polymer gas sensors. Part I: Fabrication and characterisation. Sensors and Actuators. 1989;**19**:125-140

[130] Bartlett PN, Ling-Chung SK. Conducting polymer gas sensors. Part II: Response of polypyrrole to methanol vapour. Sensors and Actuators. 1989;**19**:141-150

[131] Srivastava S, Sharma SS, Agrawal S, Kumar S, Singh M, Vijay YK. Study of chemiresistor type CNT doped polyaniline gas sensor. Synthetic Metals. 2010;**160**:529-534

[132] Xue M, Li F, Chen D, Yang Z, Wang X, Ji J. High-oriented polypyrrole nanotubes for next-generation gas sensor. Advanced Materials. 2016;**28**:8265-8270

[133] Xiang C, Jiang D, Zou Y, Chu H, Qiu S, Zhang H, et al. Ammonia sensor based on polypyrrole-graphene nanocomposite decorated with titania

nanoparticles. Ceramics International. 2015;**41**:6432-6643

[134] Hakimi M, Salehi A, Boroumand FA, Mosleh N. Fabrication of a room temperature ammonia gas sensor based on polyaniline with n-doped graphene quantum dots. IEEE Sensors Journal. 2018;**18**:2245-2252

[135] Gavgania JN, Hasanib A, Nourib M, Mahyari M, Salehi A. Highly sensitive and flexible ammonia sensor based on S and N co-doped graphene quantum dots/polyaniline hybrid at room temperature. Sensors and Actuators B: Chemical. 2016;**229**:239-248

[136] Xue L, Wang W, Guo Y, Liu G, Wan P. Flexible polyaniline/carbon nanotube nanocomposite film-based electronic gas sensors. Sensors and Actuators B. 2107;**244**:47-53

[137] Bera PS, Kundu S, Khan H, Jana S. Polyaniline coated graphene hybridized SnO_2 nanocomposite: Low temperature solution synthesis, structural property and room temperature ammonia gas sensing. Journal of Alloys and Compounds. 2018;**744**:260-270

[138] Ye Z, Jiang Y, Tai H, Yuan Z. The investigation of reduced graphene oxide/P3HT composite films for ammonia detection. Integrated Ferroelectrics. 2014;**154**:73-81

[139] Sharma HJ, Jamkar DV, Kondawar SB. Electrospun nanofibers of conducting polyaniline/Al-SnO_2 composites for hydrogen sensing applications. Procedia Materials Science. 2015;**10**:186-194

[140] Sharma S, Hussain S, Singh S, Islam SS. MWCNT-conducting polymer composite based ammonia gas sensors: A new approach for complete recovery process. Sensors and Actuators B: Chemical. 2014;**194**:213-219

[141] Joulazadeh M, Navarchian AH. Ammonia detection of one-dimensional nano-structured polypyrrole/metal oxide nanocomposites sensors. Synthetic Metals. 2015;**210**:404-411

[142] Jain S, Karmakar N, Shah A, Kothari DC, Mishra S, Shimpi NG. Ammonia detection of 1-D ZnO/polypyrrole nanocomposite: Effect of CSA doping and their structural, chemical, thermal and gas sensing behavior. Applied Surface Science. 2017;**396**:1317-1325

[143] Li Y, Jiao M, Yang M. In-situ grown nanostructured ZnO via a green approach and gas sensing properties of polypyrrole/ZnO nanohybrids. Sensors and Actuators B: Chemical. 2017;**238**:596-604

[144] Chougule MA, Sen S, Patil VB. Polypyrrole-ZnO hybrid sensor: Effect of camphor sulfonic acid doping on physical and gas sensing properties. Synthetic Metals. 2012;**162**:1598-1603

[145] Zhang D, Wu Z, Zong X, Zhang Y. Fabrication of polypyrrole/Zn_2SnO_4 nanofilm for ultrahighly sensitive ammonia sensing application. Sensors and Actuators B: Chemical. 2018;**274**:575-586

[146] Ramesan MT, Santhi V, Bahuleyan BK, Al-Maghrabi A. Structural characterization, material properties and sensor application study of in-situ polymerized polypyrrole/silver doped titanium dioxide nanocomposites. Materials Chemistry and Physics. 2018;**211**:343-354

[147] Qin Y, Cui Z, Zhang T, Liu D. Polypyrrole shell (nanoparticles)-functionalized silicon nanowires array with enhanced NH_3-sensing response. Sensors and Actuators B: Chemical. 2018;**258**:246-254

[148] Khuspe GD, Navale ST, Chougule MA, Patil VB. Ammonia gas

sensing properties of CSA doped PANi-SnO_2 nanohybrid thin films. Synthetic Metals. 2013;**185-186**:1-8

[149] Zhu G, Zhang Q, Xie G, Su Y, Zhao K, Du H, et al. Gas sensors based on polyaniline/zinc oxide hybrid film for ammonia detection at room temperature. Chemical Physics Letters. 2016;**665**:147-152

[150] Tai H, Jiang Y, Xie G, Yu J. Preparation, characterization and comparative NH_3-sensing characteristic studies of PANI/inorganic oxides nanocomposite thin films. Journal of Materials Science and Technology. 2010;**26**:605-613

[151] Tai H, Jiang Y, Xie G, Yu J, Chen X, Ying Z. Influence of polymerization temperature on NH_3 response of PANI/TiO_2 thin film gas sensor. Sensors and Actuators B: Chemical. 2008;**129**:319

[152] Li S, Lin P, Zhao L, Wang C, Liu D, Liu F, et al. The room temperature gas sensor based on polyaniline@flower-like WO_3 nanocomposites and flexible PET substrate for NH_3 detection. Sensors and Actuators B: Chemical. 2018;**259**:505-513

[153] Kulkarni S, Patil P, Mujumdar A, Naik J. Synthesis and evaluation of gas sensing properties of PANI, PANI/SnO_2 and PANI/SnO_2/rGO nanocomposites at room temperature. Inorganic Chemistry Communications. 2018;**96**:90-96

[154] Liu C, Tai H, Zhang P, Ye Z, Su Y, Jiang Y. Enhanced ammonia-sensing properties of PANI-TiO_2-Au ternary self-assembly nanocomposite thin film at room temperature. Sensors and Actuators B: Chemical. 2017;**246**:85-95

[155] Yanga X, Li L, Zhao Y. Ag/AgCl-decorated polypyrrole nanotubes and their sensory properties. Synthetic Metals. 2010;**160**:1822-1825

[156] Gong J, Li Y, Hu Z, Zhou Z, Deng Y. Ultrasensitive NH_3 gas sensor from polyaniline nanograin enchased TiO_2 fibers. Journal of Physical Chemistry C. 2010;**114**:9970-9974

[157] Patil UV, Ramgir NS, Karmakar N, Bhogale A, Debnath AK, Aswal DK, et al. Room temperature ammonia sensor based on copper nanoparticle intercalated polyaniline nanocomposite thin films. Applied Surface Science. 2015;**339**:69-74

[158] Zou Y, Wang Q, Xiang C, Tang C, Chu H, Qiu S, et al. Doping composite of polyaniline and reduced graphene oxide with palladium nanoparticles for room-temperature hydrogen-gas sensing. International Journal of Hydrogen Energy. 2016;**41**:5396-5404

[159] Xu H, Chen X, Zhang J, Wang J, Cao B, Cuid D. NO_2 gas sensing with SnO_2-ZnO/PANI composite thick film fabricated from porous nanosolid. Sensors and Actuators B: Chemical. 2013;**176**:166-173

[160] Xu H, Ju D, Li W, Gong H, Zhang J, Wang J, et al. Low-working-temperature, fast-response-speed NO_2 sensor withnanoporous-SnO_2/polyaniline double-layered film. Sensors and Actuators B: Chemical. 2016;**224**:654-660

[161] Mane AT, Navale ST, Patil VB. Room temperature NO_2 gas sensing properties of DBSA doped PPy-WO_3 hybrid nanocomposite sensor. Organic Electronics. 2015;**19**:15-25

[162] Nalage SR, Navale ST, Mane RS, Naushad M, Stadlar FJ, Patil VB. Preparation of camphor-sulfonic acid doped PPy-NiO hybrid nanocomposite for detection of toxic nitrogen dioxide. Synthetic Metals. 2015;**209**:426-433

[163] Mondal SP, Bera S, Narender G, Ray SK. CdSe quantum dots-poly(3-hexylthiophene) nanocomposite sensors

for selective chloroform vapor detection at room temperature. Applied Physics Letters. 2012;**101**:173108

[164] McDonagh C, Burke CS, MacCraith BD. Optical chemical sensors. Chemical Reviews. 2008;**108**:400-422

[165] Brédas JL, Scott JC, Yakushi K, Street GB. Polarons and bipolarons in polypyrrole: Evolution of the band structure and optical spectrum upon doing. Physical Review B. 1984;**30**:1023-1025

[166] Gallazzi MC, Tassoni L, Bertarelli C, Pioggia G, Francesco FD, Montoneri E. Poly(alkoxy-bithiophenes) sensors for organic vapours. Sensors and Actuators B: Chemical. 2003;**88**:178-189

[167] Ho CK, Itamura MT, Kelley M, Hughes RC. Review of chemical sensors for in-Situ monitoring of volatile contaminants. SAND2001-0643. Albuquerque, New Mexico: Sandia National Laboratories; 2001

[168] Hwang HR, Roh JG, Lee DD, Lim JO, Huh JS. Sensing behavior of the polypyrrole and polyaniline sensor for several volatile organic compounds. Metals and Materials International. 2003;**9**:287-291

[169] Tavoli F, Alizadeh N. Optical ammonia gas sensor based on nanostructure dye-doped polypyrrole. Sensors and Actuators B: Chemical. 2013;**176**:761-767

[170] Bansal L, El-Sherif M. Intrinsic optical-fiber sensor for nerve agent sensing. IEEE Sensors Journal. 2005;**5**:648-655

[171] Dickinson TA, White J, Kauer JS, Walt DR. A chemical-detecting system based on a cross-reactive optical sensor array. Nature. 1996;**382**:697-700

[172] Nagle HT, Gutierrez-Osuna R, Schiffman SS. The how and why of electronic noses. IEEE Spectrum. 1998;**35**:22-31

[173] El-Sherif M, Bansal L, Yuan J. Fiber optic sensors for detection of toxic and biological threats. Sensors. 2007;**7**:3100-3118

[174] Muthusamy S, Charles J, Renganathan B, Sastikumar D. In situ growth of Prussian blue nanocubes on polypyrrole nanoparticles: Facile synthesis, characterization and their application as fiber optic gas sensor. Journal of Materials Science. 2018;**53**:15401-15417

[175] Mohammed HA, Rashid AS, Baker MHA, Anas SBA, Mahdi MA, Yaacob MH. Fabrication and characterizations of a novel etched-tapered single mode optical fiber ammonia sensors integrating PANI/GNF nanocomposite. Sensors and Actuators B: Chemical. 2019;**287**:71-77

[176] Chiam YS, Lim KS, Harun SW, Gan SN, Phang SW. Conducting polymer coated optical microfiber sensor for alcohol detection. Sensors and Actuators A. 2014;**205**:58-62

[177] Qin H, Kulkarni A, Zhang H, Kimb H, Jiang D, Kim T. Polypyrrole thin film fiber optic chemical sensor for detection of VOCs. Sensors and Actuators B: Chemical. 2011;**158**:223-228

[178] Homola J, Yee SS, Gauglitz G. Surface plasmon resonance sensors: Review. Sensors and Actuators B: Chemical. 1999;**54**:3-15

[179] Homola J. Surface plasmon resonance sensors for detection of chemical and biological species. Chemical Reviews. 2008;**108**:462-493

[180] Agbor NE, Cresswell JP, Petty MC, Monkman AP. An optical gas sensor

based on polyaniline Langmuir-Blodgett films. Sensors and Actuators B: Chemical. 1997;**41**:137-141

[181] Chang SM, Muramatsu H, Nakamura C, Miyake J. The principle and applications of piezoelectric crystal sensors. Materials Science and Engineering C: Biomimetic and Supramolecular Systems. 2000;**12**:111-123

[182] Torad NL, Zhang S, Amer WA, Ayad MM, Kim M, Kim J, et al. Advanced nanoporous material-based QCM devices: A new horizon of interfacial mass sensing technology. Advanced Materials Interfaces. 2019;**6**:1900849

[183] Mujahid A, Dickert FL. Surface acoustic wave (SAW) for chemical sensing applications of recognition layers. Sensors. 2017;**17**:2716

[184] Ballantine DS, Wohltjen H. Surface acoustic wave devices for chemical analysis. Analytical Chemistry. 1989;**61**:704A-715A

[185] Shen C-Y, Cheng Y-H, Wang S-H, Kuo S-H, Hsu C-L. A polyaniline/WO_3 nanocomposite layer based surface acoustic wave NO_2 gas sensors. In: ICICIC. 2010. pp. 1220-1222

[186] Sadek AZ, Wlodarski W, Shin K, Kaner RB, Kalantar-Zadeh K. A layered surface acoustic wave gas sensor based on a polyaniline/In_2O_3 nanofibre composite. Nanotechnology. 2006;**17**:4488-4492

[187] Shen CY, Huang HM, Wang SH, Chiu YC. Room temperature detection properties of a surface acoustic wave gas sensor with Cu^{2+}/PANI/SnO_2 nanocomposite thin film to nitric oxide. Applied Mechanics and Materials. 2013;**312**:732-735

[188] Wang B, Zheng L, Zhou L. Surface acoustic wave sensors with graphene/PANI nanocomposites for nitric oxide detection. IOP Conference Series: Earth and Environmental Science. 2017;**100**:012044

[189] Milella E, Penza M. SAW gas detection using Langmuir-Blodgett polypyrrole films. Thin Solid Films. 1998;**329**:694-697

[190] Penza M, Milella E, Anisimkin VI. Monitoring of NH_3 gas by LB polypyrrole-based SAW sensor. Sensors and Actuators B: Chemical. 1998;**47**:218-224

[191] Penza M, Milella E, Anisimkin VI. Gas sensing properties of Langmuir-Blodgett polypyrrole film investigated by surface acoustic waves. IEEE Transactions on Ultrasonics, Ferroelectrics, and Frequency Control. 1998;**45**:1125-1132

[192] Yan XF, Li DM, Hou CC, Wang X, Zhou W, Liu M, et al. Comparison of response towards NO_2 and H_2S of PPy and PPy/TiO_2 as SAW sensitive films. Sensors and Actuators B. 2012;**161**:329-333

[193] Hillier AC, Ward MD. Scanning electrochemical mass sensitivity mapping of the quartz crystal microbalance in liquid media. Analytical Chemistry. 1992;**64**:2539-2554

[194] Tang J, Torad NL, Salunkhe RR, Yoon J-H, Al Hossain MS, Dou SX, et al. Towards vaporized molecular discrimination: A quartz crystal microbalance (QCM) sensor system using cobalt-containing mesoporous graphitic carbon. Chemistry, an Asian Journal. 2014;**9**:3238-3244

[195] Sauerbrey G. Verwendung von Schwingquarzen zur Wägung dünner Schichten und zur Mikrowägung. Zeitschrift für Physik. 1959;**155**:206-222

[196] King WH. Piezoelectric sorption detector. Analytical Chemistry. 1964;**36**:1735-1739

[197] Watts ET, Krim J, Widom A. Experimental observation of interfacial slippage at the boundary of molecularly thin films with gold substrates. Physical Review B. 1990;**41**:3466

[198] Ayad MM, Salahuddin NA, Shenashin MA. Optimum reaction conditions for in situ polyaniline films. Synthetic Metals. 2003;**132**:185-190

[199] Ayad MM, Gemaey AH, Salahuddin NA, Shenashin MA. The kinetics and spectral studies of the in situ polyaniline film formation. Journal of Colloid and Interface Science. 2003;**263**:196-201

[200] Ayad MM. In-situ polypyrrole film formation using ferric nitrate as oxidizing agent. Journal of Materials Science. 2003;**22**:1577-1579

[201] Ayad MM, Rehab AF, El-Hallag IS, Amer WA. Preparation and characterization of polyaniline films in the presence of N-phenyl-1, 4-phenylenediamine. European Polymer Journal. 2007;**43**:2540-2549

[202] Abbas MN, Moustafa GA, Mitrovics J, Gopel W. Multicomponent gas analysis of a mixture of chloroform, octane and toluene using a piezoelectric quartz crystal sensor array. Analytica Chimica Acta. 1999;**393**:67-76

[203] Ide J, Nakamoto T, Moriizumi T. Development of odour-sensing system using an auto-sampling stage. Sensors and Actuators A. 1993;**13**:351-354

[204] Xu X, Cang H, Li C, Zhao ZK, Li H. Quartz crystal microbalance sensor array for the detection of volatile organic compounds. Talanta. 2009;**78**:711-716

[205] Açikbaş Y, Evyapan M, Ceyhan T, ÇaPan R, Bekaroğlu Ö. Characterization and organic vapor sensing properties of Langmuir-Blodgett film using a new three oxygen-linked phthalocyanine incorporating lutetium. Sensors and Actuators B: Chemical. 2009;**135**:426-429

[206] Gomes MTSR, Veríssimo MIS, Oliveira JABP. Detection of volatile amines using a quartz crystal with gold electrodes. Sensors and Actuators B: Chemical. 1999;**57**:261-267

[207] Ayad MM, Torad NL, Minisy IM, Izriq R, Ebeid EM. A wide range sensor of a 3D mesoporous silica coated QCM electrodes for the detection of volatile organic compounds. Journal of Porous Materials. 2019;**26**:1731-1741

[208] Ayad MM, Salahuddin NA, Abu El-Nasr A, Torad NL. Amine-functionalized mesoporous silica KIT-6 as a controlled release drug delivery carrier. Microporous and Mesoporous Materials. 2016;**229**:166-177

[209] Ayad MM, Salahuddin NA, Torad NL, Abu El-Nasr A. pH-responsive sulphonated mesoporous silica: A comparative drug release study. RSC Advances. 2016;**6**:57929-57940

[210] Ayad MM, Minisy IM. Detection and kinetics of methylamine on chitosan film coated quartz crystal microbalance electrode. Progress in Organic Coating. 2016;**100**:76-80

[211] Ayad MM, Salahuddin NA, Minisy IM. Detection of some volatile organic compounds with chitosan-coated quartz crystal microbalance. Designed Monomers and Polymers. 2014;**17**:795-802

[212] Ayad MM, Abu El-Nasr A. Adsorption of cationic dye (methylene blue) from water using polyaniline nanotubes base. Journal of Physical Chemistry C. 2010;**114**:14377-14383

[213] Ayad MM, El-Hefnawey G, Torad NL. Quartz crystal microbalance sensor coated with polyaniline emeraldine base for determination of chlorinated aliphatic hydrocarbons. Sensors and Actuators B: Chemical. 2008;**134**:887-894

[214] Ayad MM, Torad NL. Alcohol vapours sensor based on thin polyaniline salt film and quartz crystal microbalance. Talanta. 2009;**78**:1280-1285

[215] Ayad MM, El-Hefnawey G, Torad NL. A sensor of alcohol vapours based on thin polyaniline base film and quartz crystal microbalance. Journal of Hazardous Materials. 2009;**168**:85-88

[216] Ayad MM, Salahuddin NA, Minisy IM, Amer WA. Chitosan/polyaniline nanofibers coating on the quartz crystal microbalance electrode for gas sensing. Sensors and Actuators B: Chemical. 2014;**202**:144-153

[217] Ayad MM, Torad NL. Quartz crystal microbalance sensor for detection of aliphatic amines vapours. Sensors and Actuators B: Chemical. 2010;**147**:481-487

[218] Crank J. The Mathematics of Diffusion. 2nd ed. Oxford: Clarendon Press; 1975. p. 414

[219] Li G, Zheng J, Ma X, Sun Y, Fu J, Wu G. Development of QCM trimethylamine sensor based on water soluble polyaniline. Sensors. 2007;**7**:2378-2388

[220] Zheng J, Li G, Ma X, Wang Y, Wu G, Cheng Y. Polyaniline-TiO_2 nanocomposite-based trimethylamine QCM sensor and its thermal behavior studies. Sensors and Actuators B: Chemical. 2008;**133**:374-380

[221] Ihdene Z, Mekki A, Mettai B, Mahmoud R, Hamada B, Chehimi MM. Quartz crystal microbalance VOCs sensor based on dip coated polyaniline emeraldine salt thin films. Sensors and Actuators B: Chemical. 2014;**203**:647-654

[222] Xu L, Hu X, Lim YT, Subramanian VS. Organic vapor adsorption behavior of poly(3-butoxythiophene) LB films on quartz crystal microbalance. Thin Solid Films. 2002;**417**:90-94

[223] Cui S, Yang L, Wang J, Wang X. Fabrication of a sensitive gas sensor based on PPy/TiO_2 nanocomposites films by layer-by-layer self-assembly and in food storage. Sensors and Actuators B: Chemical. 2016;**233**:337-346

[224] Su P-G, Chang Y-P. Low-humidity sensor based on a quartz-crystal microbalance coated with polypyrrole/Ag/TiO_2 nanoparticles composite thin films. Sensors and Actuators B: Chemical. 2008;**129**:915-920

[225] Zhang D, Wang D, Zong X, Dong G, Zhang Y. High-performance QCM humidity sensor based on graphene oxide/tin oxide/polyaniline ternary nanocomposite prepared by in-situ oxidative polymerization method. Sensors and Actuators B: Chemical. 2018;**262**:531-541

[226] Zhang D, Wang D, Li P, Zhou X, Zong X, Dong G. Facile fabrication of high-performance QCM humidity sensor based on layer-by-layer self-assembled polyaniline/graphene oxide nanocomposite film. Sensors and Actuators B: Chemical. 2018;**255**:1869-1877